

## Supporting Information

### **Rapid, Ambient Temperature Synthesis of Imine Covalent Organic Frameworks Catalyzed by Transition-Metal Nitrates**

Dongyang Zhu,<sup>1</sup> Zhuqing Zhang,<sup>1</sup> Lawrence B. Alemany,<sup>2</sup> Yilin Li,<sup>1</sup> Njideka Nnorom,<sup>1</sup> Morgan Barnes,<sup>3</sup> Safiya Khalil,<sup>1</sup> Muhammad M. Rahman,<sup>3</sup> Pulickel M. Ajayan<sup>3</sup> and Rafael Verduzco<sup>\*,1,3</sup>

[1] Department of Chemical and Biomolecular Engineering, Rice University, 6100 Main Street, MS-362, Houston, Texas 77005, United States

[2] Shared Equipment Authority and Department of Chemistry, Rice University, 6100 Main Street, Houston, TX, 77005, USA

[3] Department of Materials Science and NanoEngineering, Rice University, 6100 Main Street, MS-325, Houston, Texas 77005, United States

Corresponding author: Professor Rafael Verduzco, [rafaelv@rice.edu](mailto:rafaelv@rice.edu)

## Section 1. Synthesis

### COF Synthesis

#### Part 1. Synthesis of TAPB-OMePDA COF using different catalysts for 2 hours or 3 days

TAPB (20.9 mg, 0.059 mmol) and OMePDA (17.3 mg, 0.089 mmol) were weighed and dissolved in a mixture of 1 mL DCB and 1 mL 1-butanol in a 4 mL glass vial directly. The vial was sonicated for a while until all particles dissolved in the solvents. Then 5mol% of different catalysts (Fe-NO, Ni-NO, Mn-NO, Zn-NO, Cu-NO, Co-NO) were weighed and added. The molar percent is based on the total amount of amine groups. For example, TAPB has three amine groups in the single structure, so 0.059 mmol TAPB contains 0.177 mmol amine groups. Later, the vial was sonicated again for a while and placed still for 2 hours or 3 days. One point worth mentioning is that 1-butanol was found to effectively dissolve metal nitrates and combination of DCB/1-butanol served as effective reaction solvents, while another common solvent combination (dioxane/mesitylene) did not produce crystalline samples.

All products were separated and washed thoroughly using THF/water, acetone and ethanol. Being washed using large excess of water is important to remove any of the water-soluble metal nitrate catalysts. In order to exclude the possibility of pore collapse and yield dry COF powders with similar pore structures as grown, ScCO<sub>2</sub> drying for all samples was employed. Supercritical CO<sub>2</sub> drying was conducted on a Leica EM CPD300 automated Critical Point Dryer. Wetted COF powders were loaded in tea bags and then transferred into the dryer chambers with addition of appropriate amount of pure ethanol.

The isolated yields using different catalysts after 2 hours are 92.0% (Fe-NO), 87.5% (Ni-NO), 88.2% (Mn-NO), 87.1% (Zn-NO), 86.3% (Cu-NO) and 82.4% (Co-NO), respectively. The isolated yields using different catalysts after 3 days are 93.4% (Fe-NO), 87.2% (Ni-NO), 88.7% (Mn-NO), 86.8% (Zn-NO), 83.5% (Cu-NO) and 83.3% (Co-NO), respectively.

#### Part 2. Synthesis of TAPB-OMePDA COF using different equivalents of Fe-NO for 2 hours

All procedures are same as **part 1** except using different molar equivalents of Fe-NO (1 mol%, 2 mol%, 3 mol%, 5 mol%, 7 mol%, 10 mol%). The isolated yields using different equivalents of Fe-NO are 87.9% (1 mol% Fe-NO), 86.8% (2 mol% Fe-NO), 88.2% (3 mol% Fe-NO), 92.2% (5 mol% Fe-NO), 90.3% (7 mol% Fe-NO) and 92.5% (10 mol% Fe-NO), respectively.

### Part 3. Synthesis of TAPB-OMePDA COF using 10mol% of Fe-NO for different times

All procedures are same as **part 1** except using 10 mol% of Fe-NO for different times (10 min, 20 min, 30 min, 60 min, 90 min, 120 min). The isolated yields using 10 mol% Fe-NO after different times are 76.3% (10 min), 85.9%(20 min), 87.2% (30 min), 87.7% (60 min), 89.5% (90 min) and 92.3% (120 min), respectively.

### Part 4. General synthesis of different COFs (Scheme S1-S6) using 10 mol% of Fe-NO for 2 hours

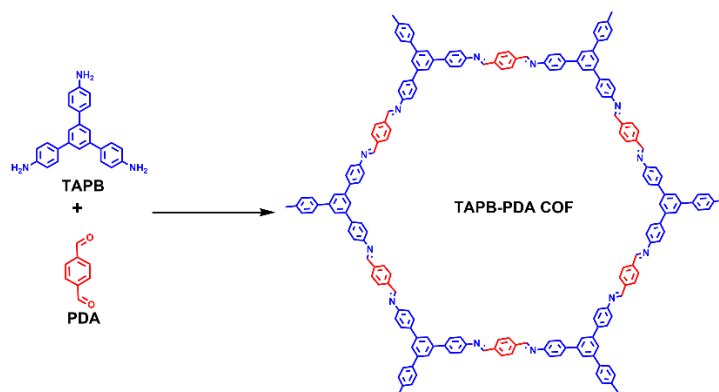
All procedures are same as **part 1** except using 10mol% of Fe-NO to react for 2 hours. The isolated yields for different COFs are 88.4% (TAPB-PDA), 87.6% (TAPB-BPDA), 76.7% (COF-V), 91.5% (TAPB-C8PDA), 62.0% (TAPT-PDA), and 93.1% (TAPT-OMePDA), respectively.

### Part 5. Solvothermal synthesis of TAPT-PDA COF using acetic acid for 3 days

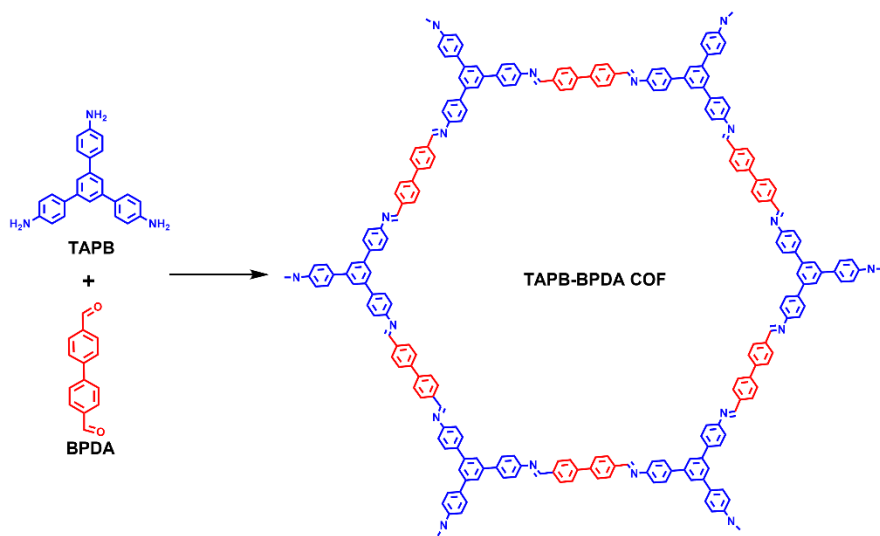
TAPT (25.5 mg, 0.072 mmol) and PDA (14.5 mg, 0.108 mmol) were weighed and dissolved in a mixture of 1.6 mL of dioxane and 0.4 mL of mesitylene in a Pyrex tube directly. Before the tube was sealed, 0.2 mL of 6 M acetic acid was added and the solution was sonicated for 10 min. The sealed tubes were transferred into oven and heated to 120 °C for 3 days. All of the products were separated and washed thoroughly using THF and ethanol, and then were dried using ScCO<sub>2</sub> drying. We also optimized solvent combinations (table S1), but none of the samples show crystallinity.

**Table S1.** Solvent combinations used to synthesize TAPT-PDA COFs using solvothermal methods

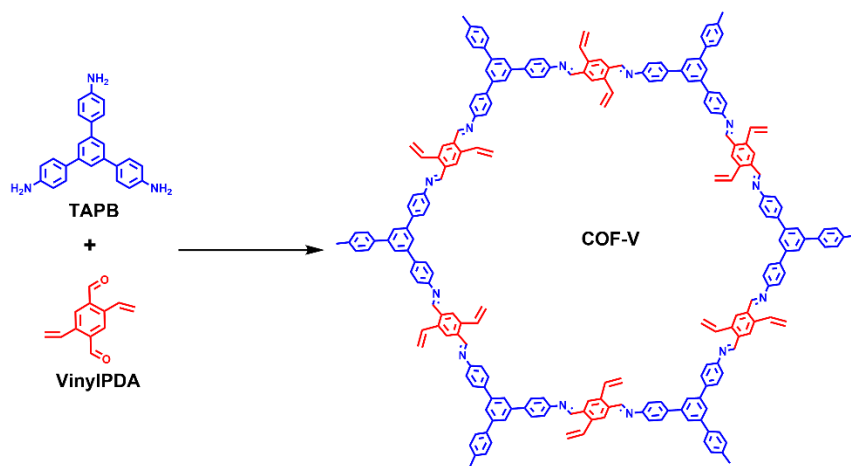
No.	Solvent	Solvent
1	Dioxane=1.8 ml	Mesitylene=0.2 ml
2	Dioxane=1.6 ml	Mesitylene=0.4 ml
3	Dioxane=1.2 ml	Mesitylene=0.8 ml
4	Dioxane=1 ml	Mesitylene=1 ml
5	Dioxane=0.5 ml	Mesitylene=1.5 ml
6	Dioxane=0.2 ml	Mesitylene=1.8 ml
7	DCB=0.5 ml	1-butanol=1.5 ml
8	DCB=1 ml	1-butanol=1 ml
9	DCB=1.5 ml	1-butanol=0.5 ml



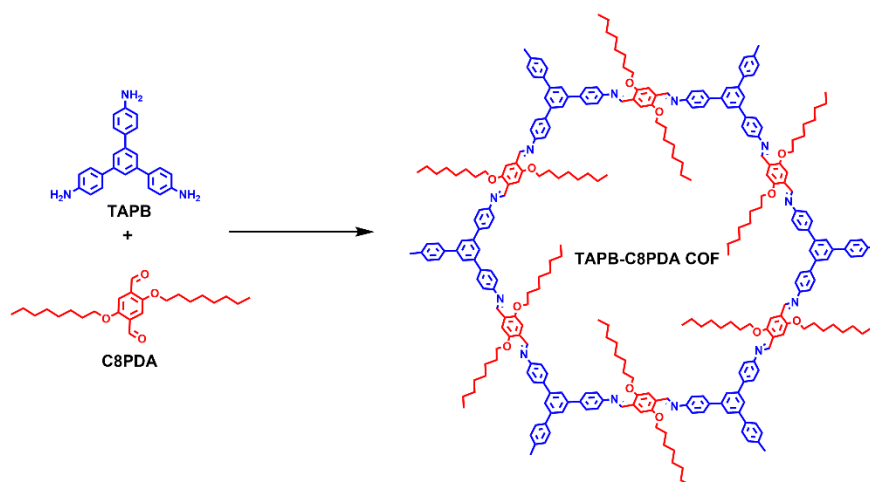
**Scheme S1.** Synthesis of TAPB-PDA COF



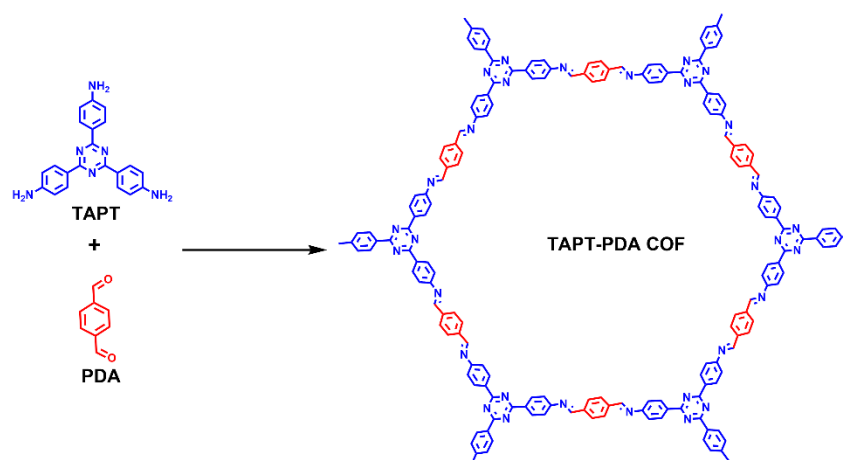
**Scheme S2.** Synthesis of TAPB-BPDA COF



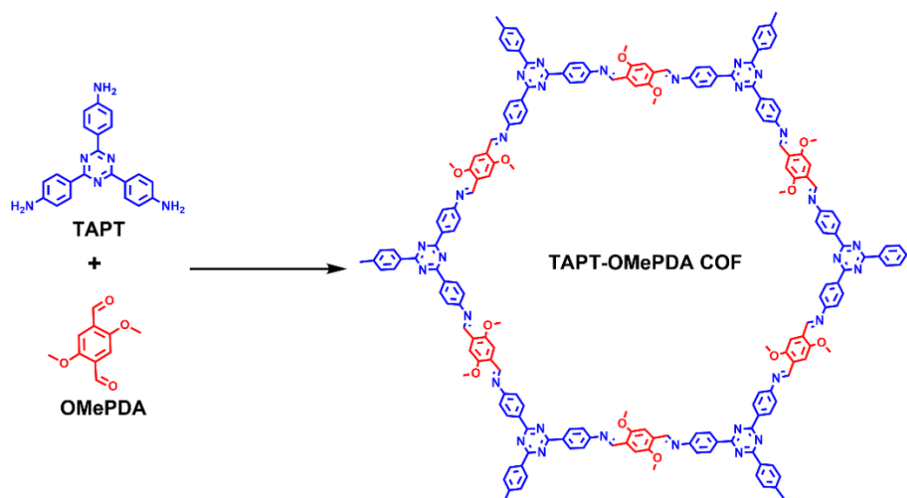
**Scheme S3.** Synthesis of COF-V



**Scheme S4.** Synthesis of TAPB-C8PDA COF

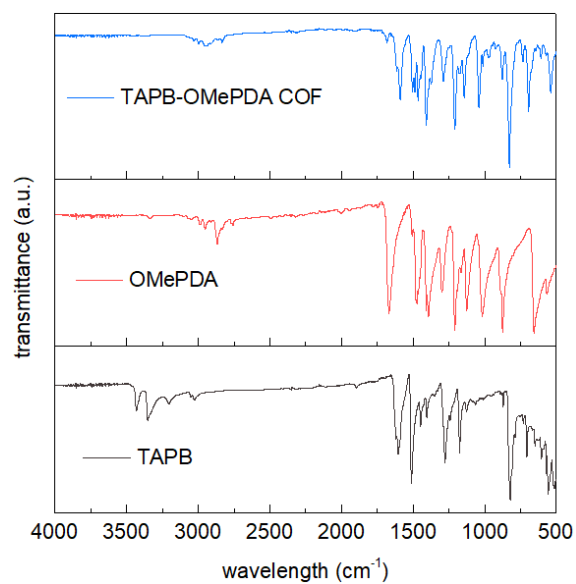


**Scheme S5.** Synthesis of TAPT-PDA COF

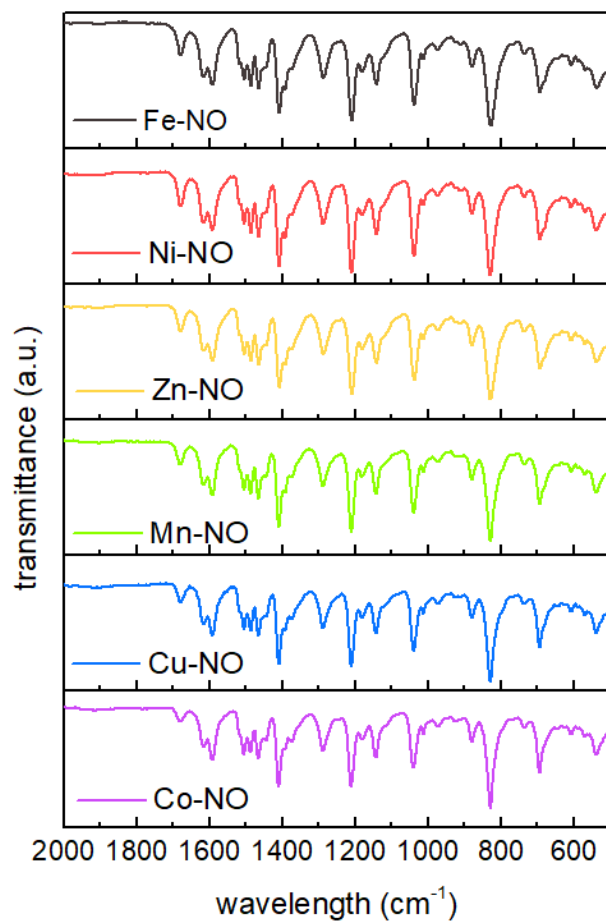


**Scheme S6.** Synthesis of TAPT-OMePDA COF

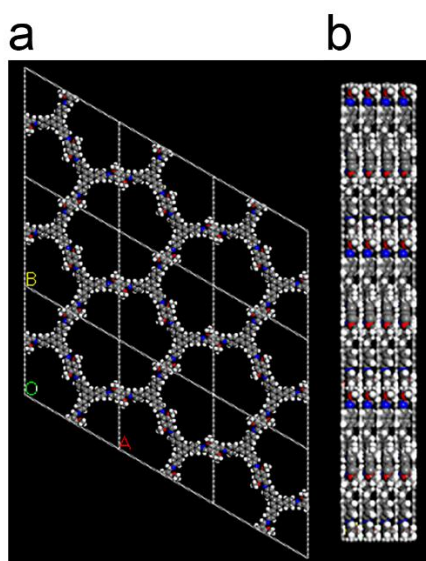
## Section 2. Additional data



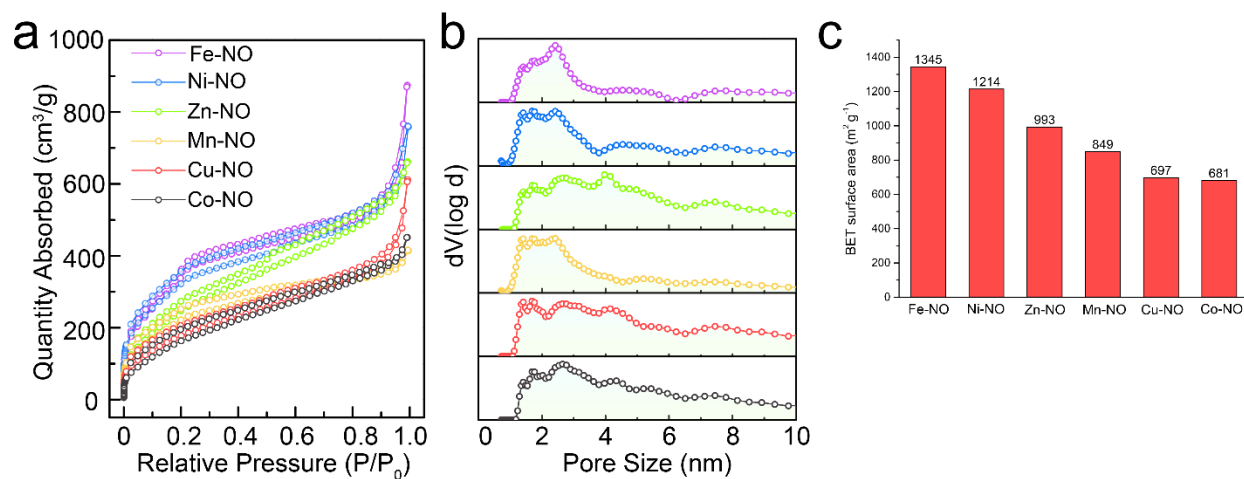
**Figure S1.** FT-IR spectra of TAPB-OMePDA COF synthesized using Fe-NO for 2 hours and corresponding monomers—TAPB and OMePDA.



**Figure S2.** FT-IR spectra of TAPB-OMePDA COFs synthesized using different catalysts for 2 hours

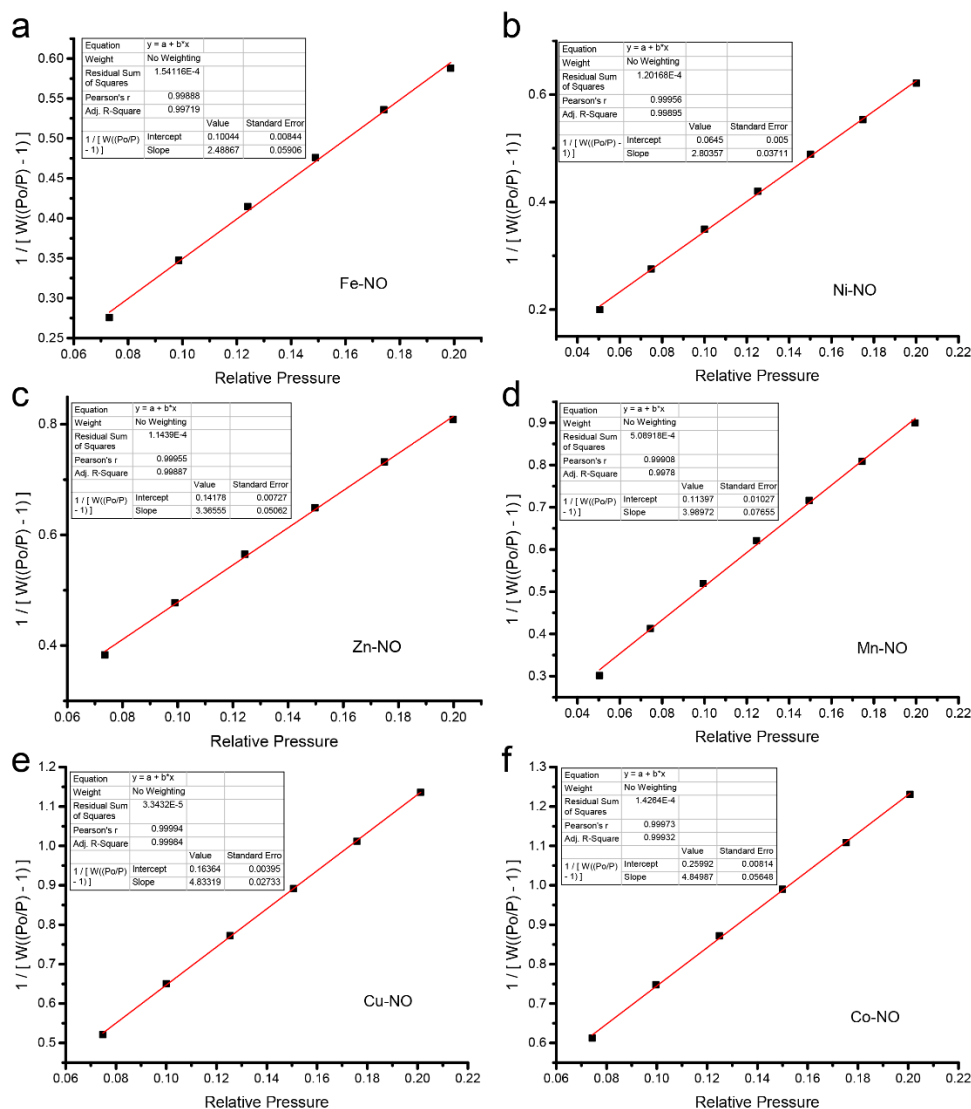


**Figure S3.** TAPB-OMePDA COF structure (AA-stacking)



**Figure S4.** (a) Nitrogen sorption tests, (b) the corresponding pore size distributions, and (c) BET surface areas of TAPB-OMePDA COFs synthesized with different catalysts for 2 hours

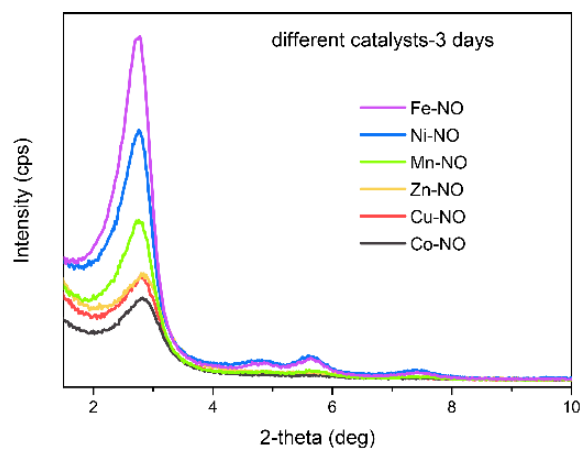




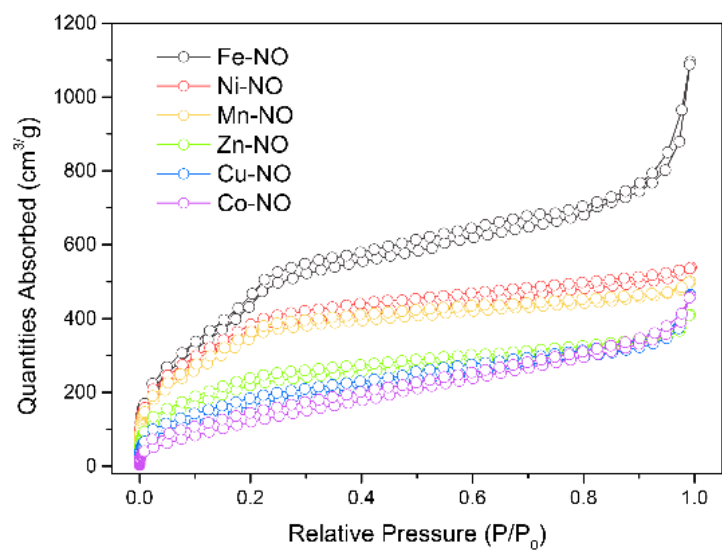
**Figure S5.** BET surface areas calculation---t plots for TAPB-OMePDA COF synthesized with different catalysts for 2 hours

Table S2 FWHM values for TAPB-OMePDA COFs synthesized using different catalysts for 2hours

Transition metal nitrates	FWHM (degree)
Fe-NO	0.73
Ni-NO	0.78
Zn-NO	0.79
Mn-NO	0.80
Cu-NO	0.90
Co-NO	1.02



**Figure S6.** PXRD spectra of TAPB-OMePDA COFs synthesized with different catalysts for 3 days



**Figure S7.** Nitrogen sorption isotherms of TAPB-OMePDA COFs synthesized with different catalysts for 3 days

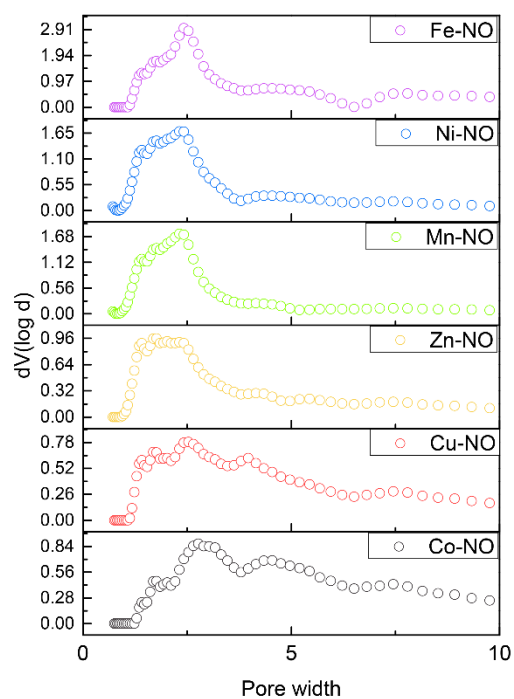


**Figure S8.** Pore size distributions for TAPB-OMePDA COFs synthesized with different catalysts for 3 days

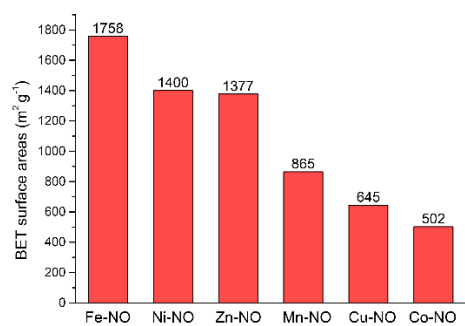


**Figure S9.** BET surface areas of TAPB-OMePDA COFs synthesized with different catalysts for 3 days

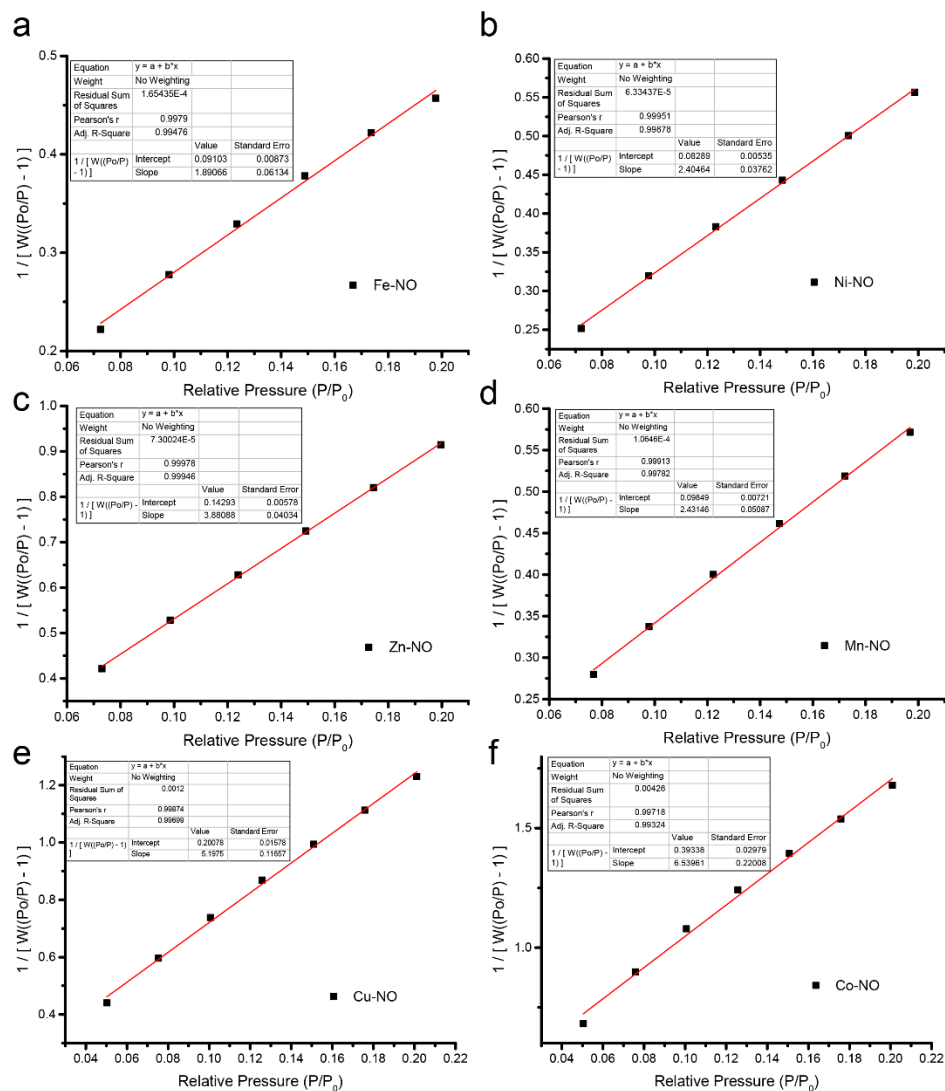


**Figure S10.** BET surface areas calculation---t plots for TAPB-OMePDA COF synthesized with different catalysts for 3 days

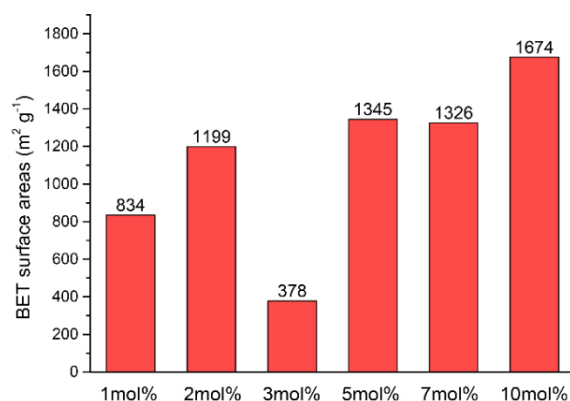


**Figure S11.** BET surface areas of TAPB-OMePDA COFs synthesized using different equivalents of Fe-NO for 2 hours

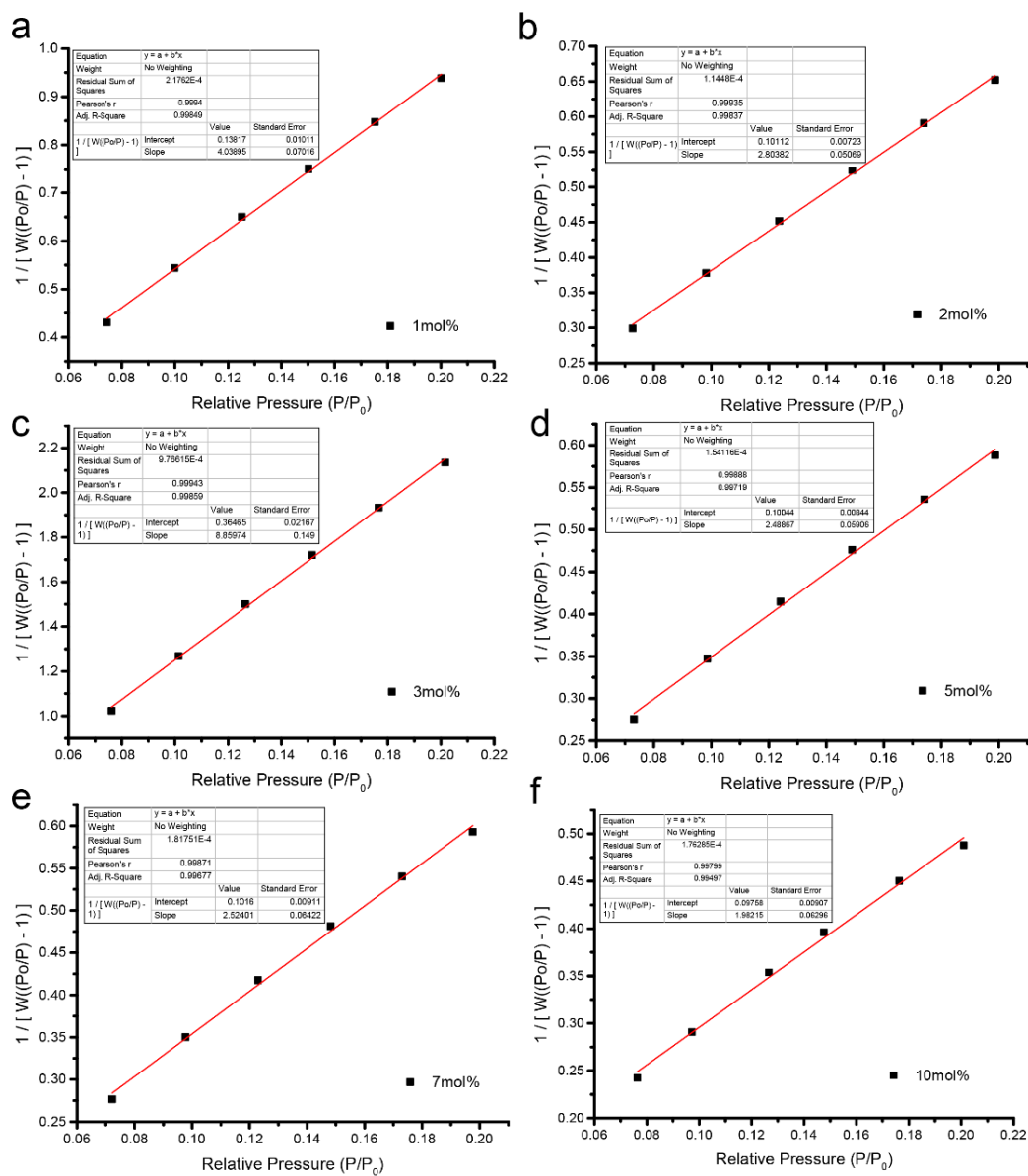


**Figure S12.** BET surface area calculations---t plots for TAPB-OMePDA COF synthesized using different equivalents of Fe-NO for 2 hours

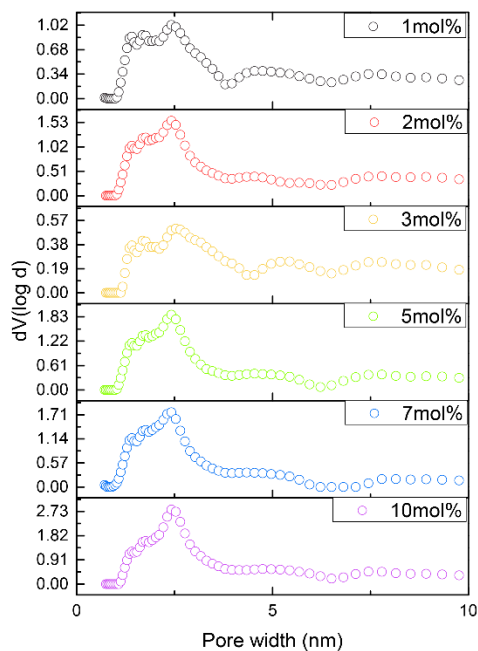


**Figure S13.** Pore size distributions of TAPB-OMePDA COF synthesized using different loadings of Fe-NO and for a reaction time of 2 hours

#### XPS studies to analyze the existence of iron element

XPS survey spectrum was first studied and no obvious iron peak was observed, meaning that the total iron percentage in the final COF sample was very low. To confirm the element ratio of iron, high resolution element XPS was conducted and the final ratio of iron was calculated as 0.02 atomic% (atomic percent, C 83.36%, N 5.98%, O 10.63%).

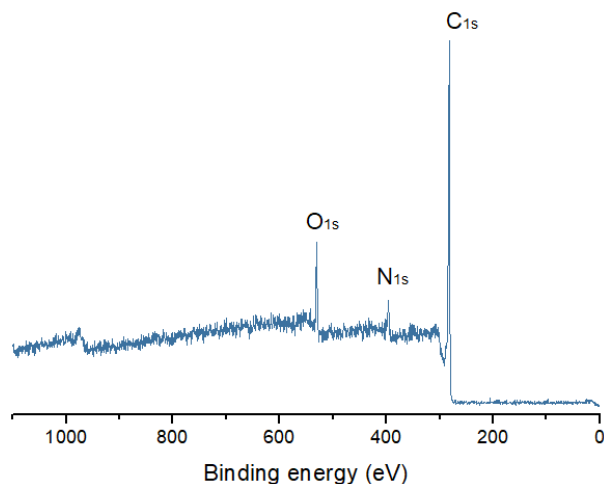


**Figure S14.** XPS survey spectrum for TAPB-OMePDA COF prepared using 10 mol% Fe-NO

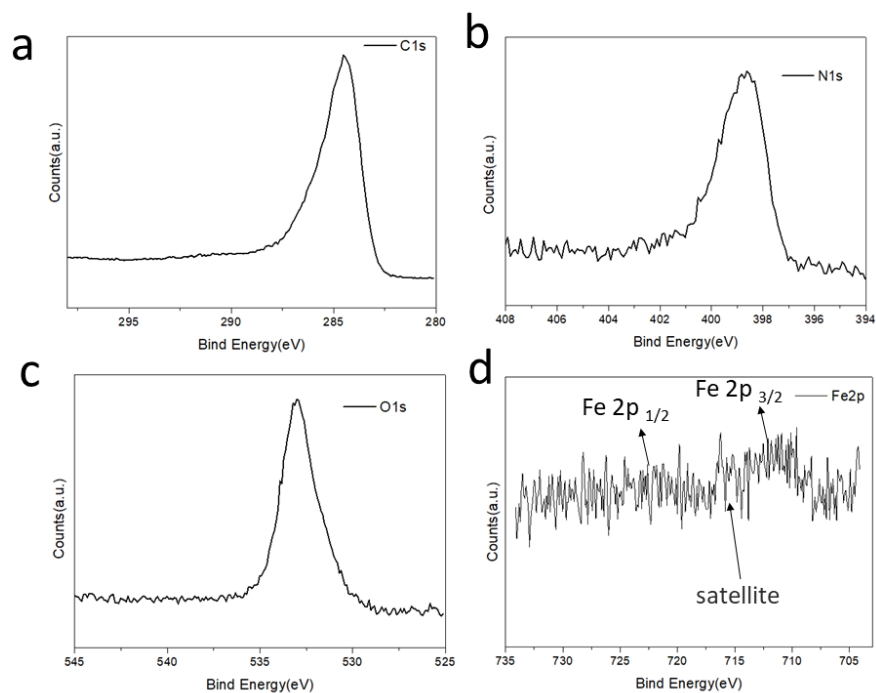


**Figure S15.** High resolution C1s, N1s, O1s and Fe2p XPS spectrum for TAPB-OMePDA COF prepared using 10 mol% Fe-NO

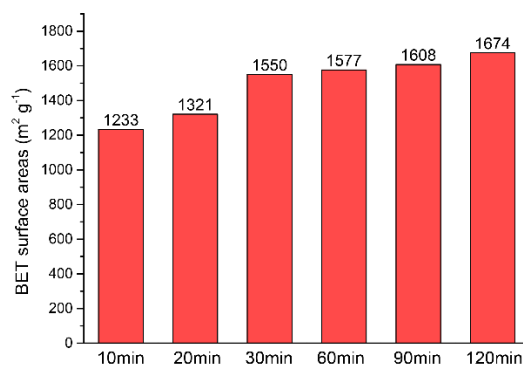


**Figure S16.** BET surface areas of TAPB-OMePDA COFs synthesized using 10 mol% Fe-NO for different times

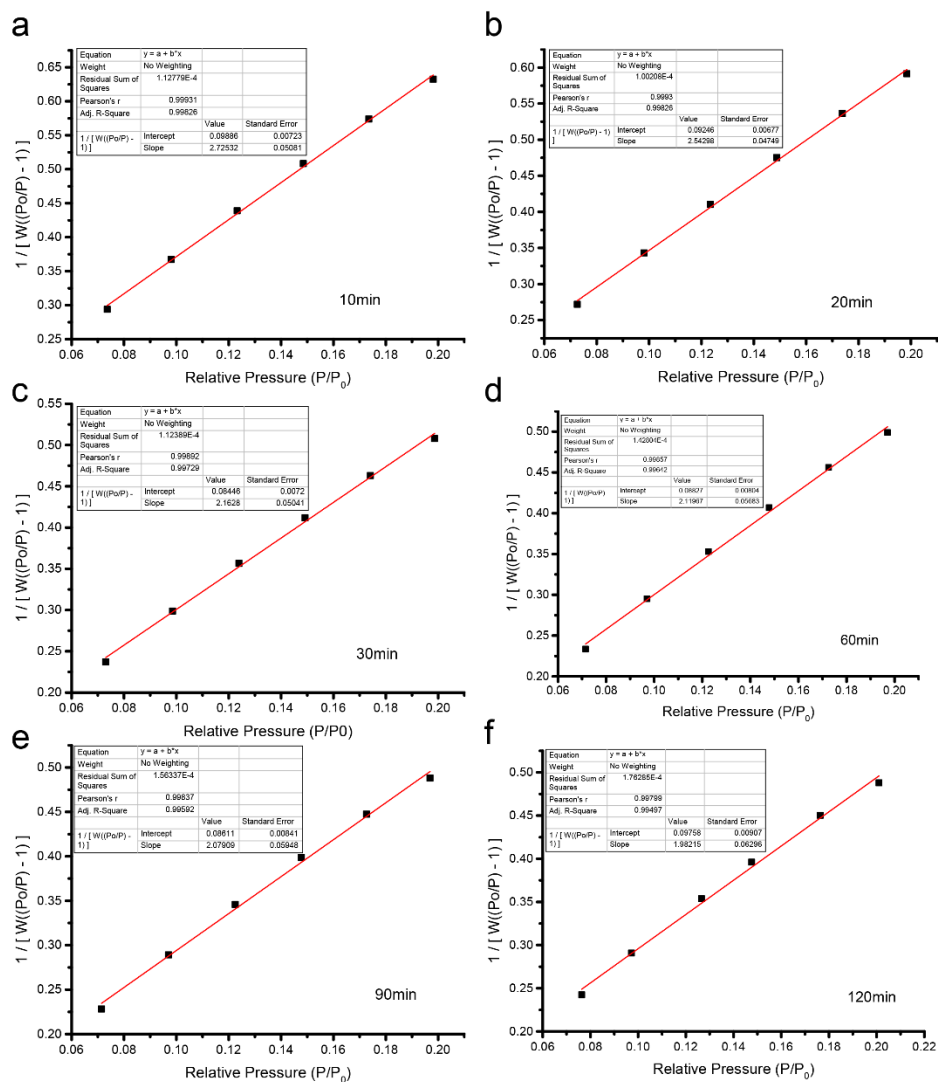


**Figure S17.** BET surface area calculations---t plot for TAPB-OMePDA COF synthesized using 10 mol% of Fe-NO for different times



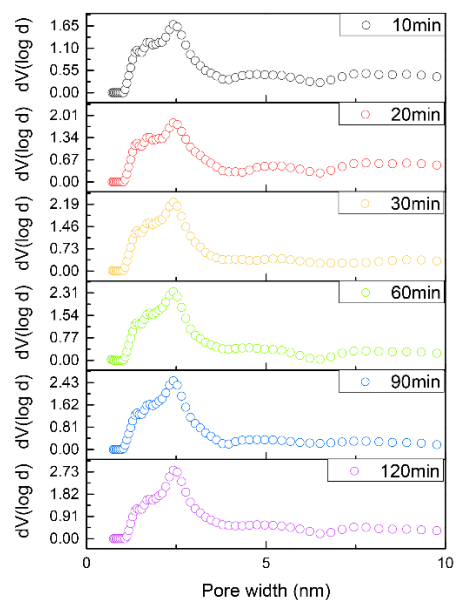


**Figure S18.** Pore size distributions of TAPB-OMePDA COF synthesized using 10mol% of Fe-NO for different times

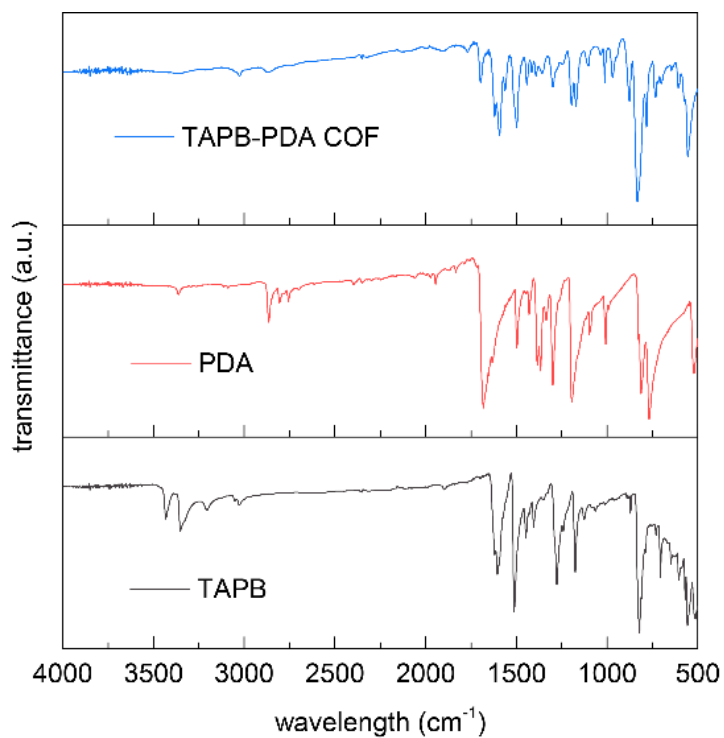


**Figure S19.** FT-IR spectra of TAPB-PDA COF by using 10 mol% Fe-NO as catalyst for 2 hours and their corresponding monomers--- TAPB and PDA.

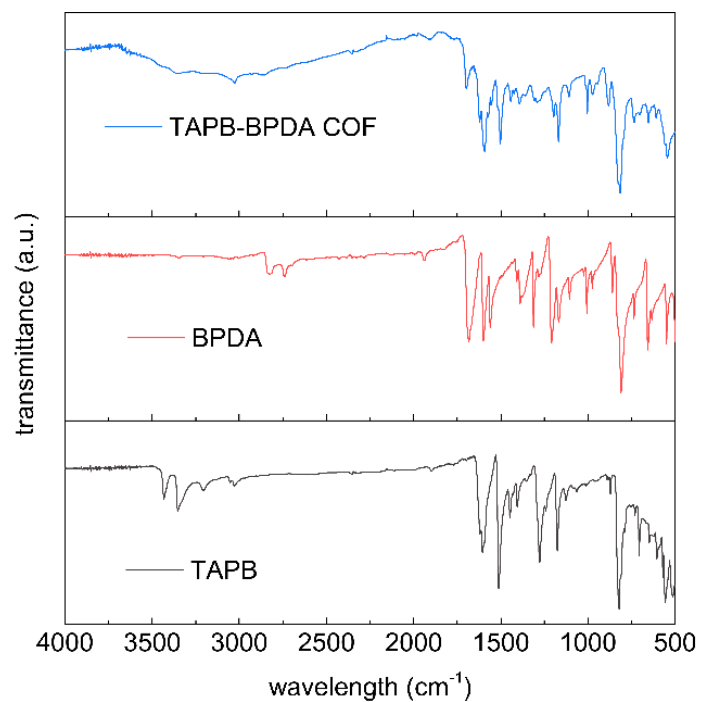


**Figure S20.** FT-IR spectra of TAPB-BPDA COF by using 10 mol% Fe-NO as catalyst for 2 hours and their corresponding monomers--- TAPB and BPDA.

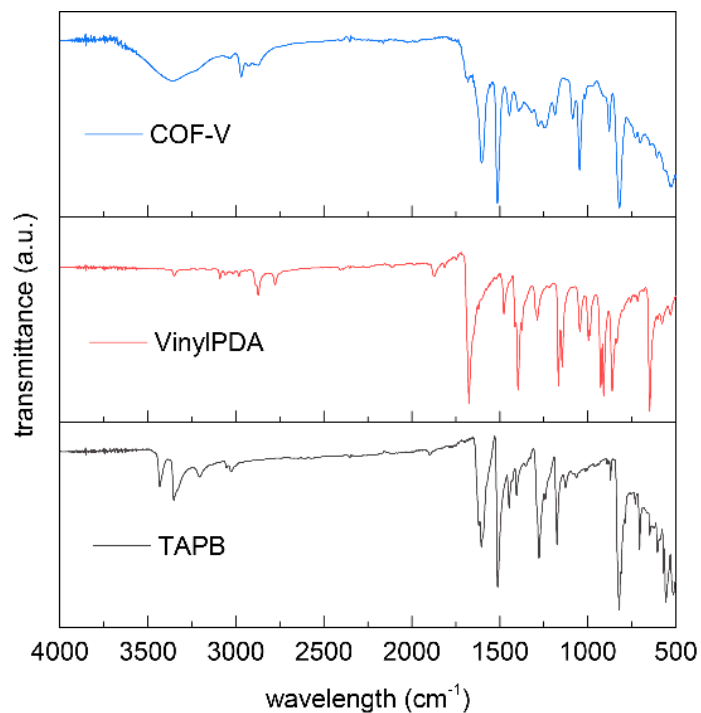


**Figure S21.** FT-IR spectra of COF-V by using 10 mol% Fe-NO as catalyst for 2 hours and their corresponding monomers--- TAPB and vinylPDA.

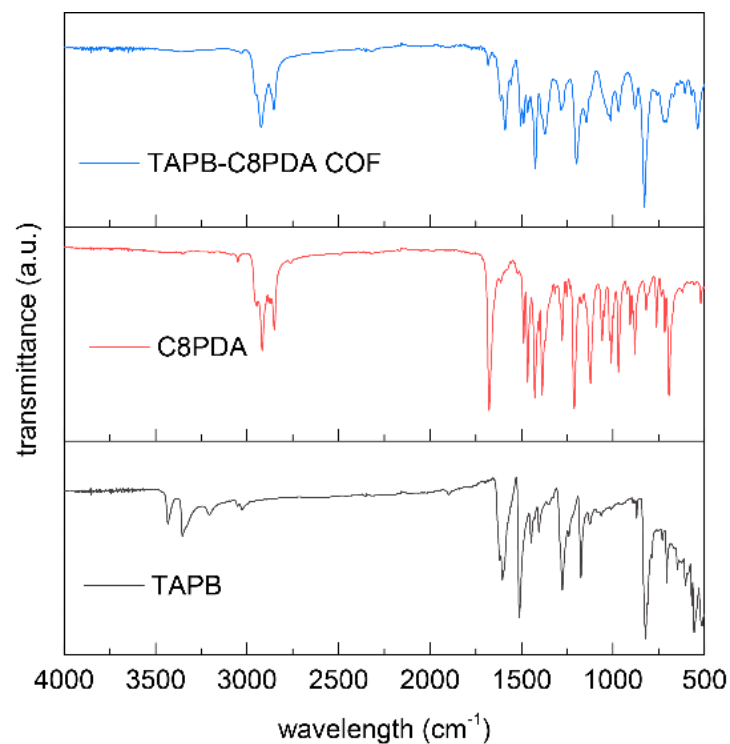


**Figure S22.** FT-IR spectra of TAPB-C8PDA COF by using 10 mol% Fe-NO as catalyst for 2 hours and their corresponding monomers--- TAPB and C8PDA.

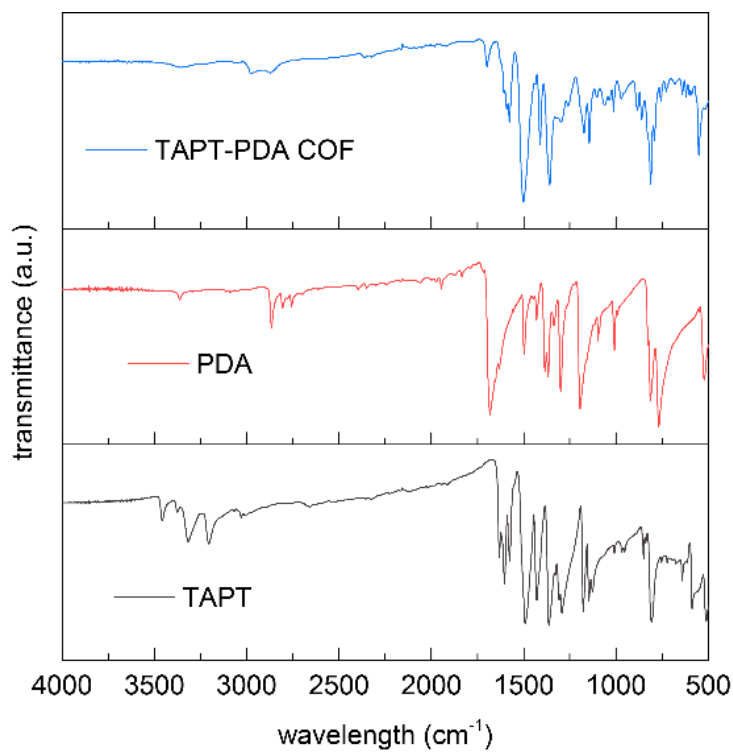


**Figure S23.** FT-IR spectra of TAPT-PDA COF by using 10 mol% Fe-NO as catalyst for 2 hours and their corresponding monomers--- TAPT and PDA.

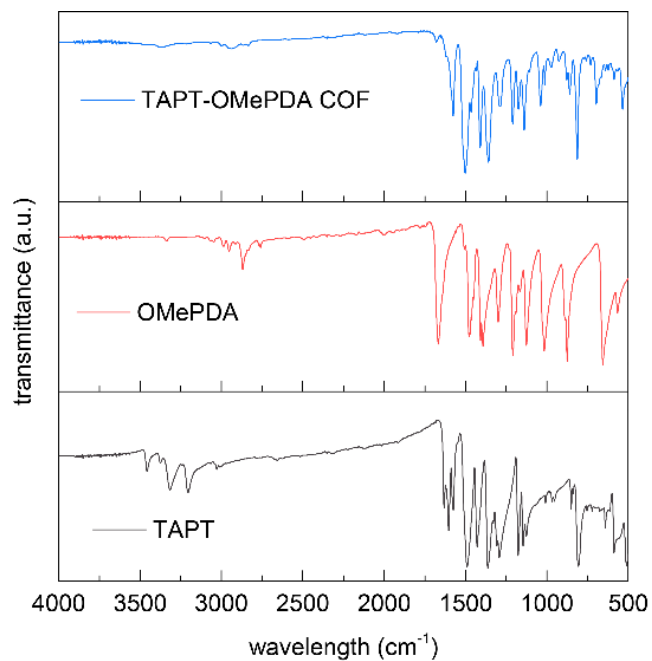


**Figure S24.** FT-IR spectra of TAPT-OMePDA COF by using 10 mol% Fe-NO as catalyst for 2 hours and their corresponding monomers--- TAPT and OMePDA.

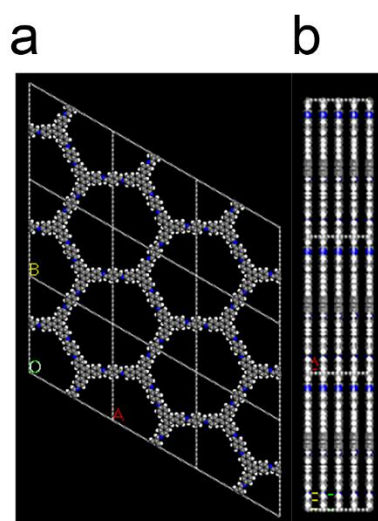


**Figure S25.** Simulated structures of TAPB-PDA COF (AA-stacking)

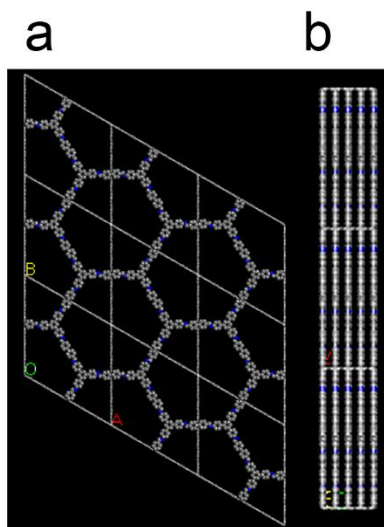


**Figure S26.** Simulated structures of TAPB-BPDA COF (AA-stacking)

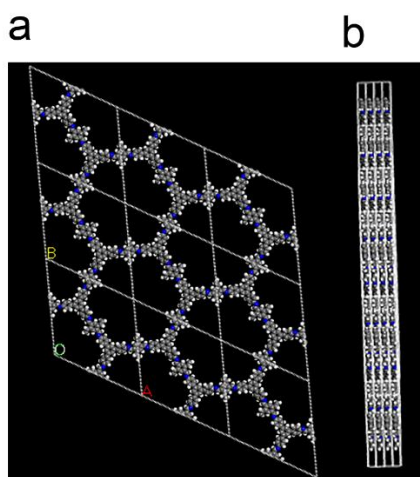


**Figure S27.** Simulated structures of COF-V (AA-stacking)

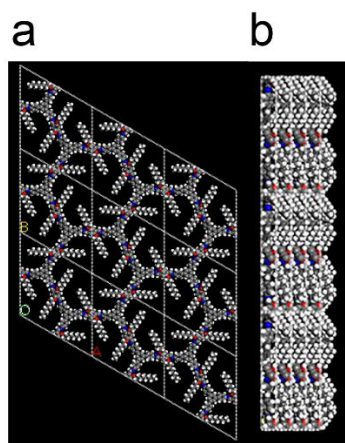


**Figure S28.** Simulated structures of TAPB-C8PDA COF (AA-stacking)

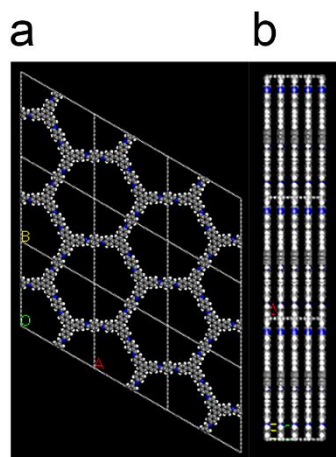


**Figure S29.** Simulated structures of TAPT-PDA COF (AA-stacking)

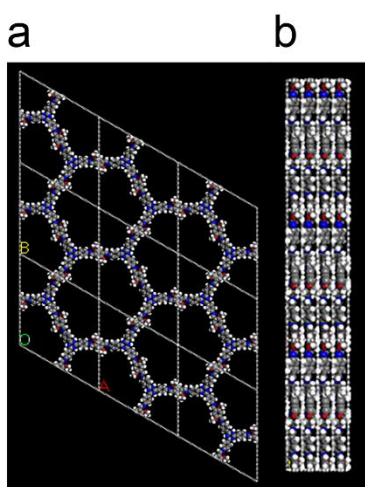


**Figure S30.** Simulated structures of TAPT-OMePDA COF (AA-stacking)

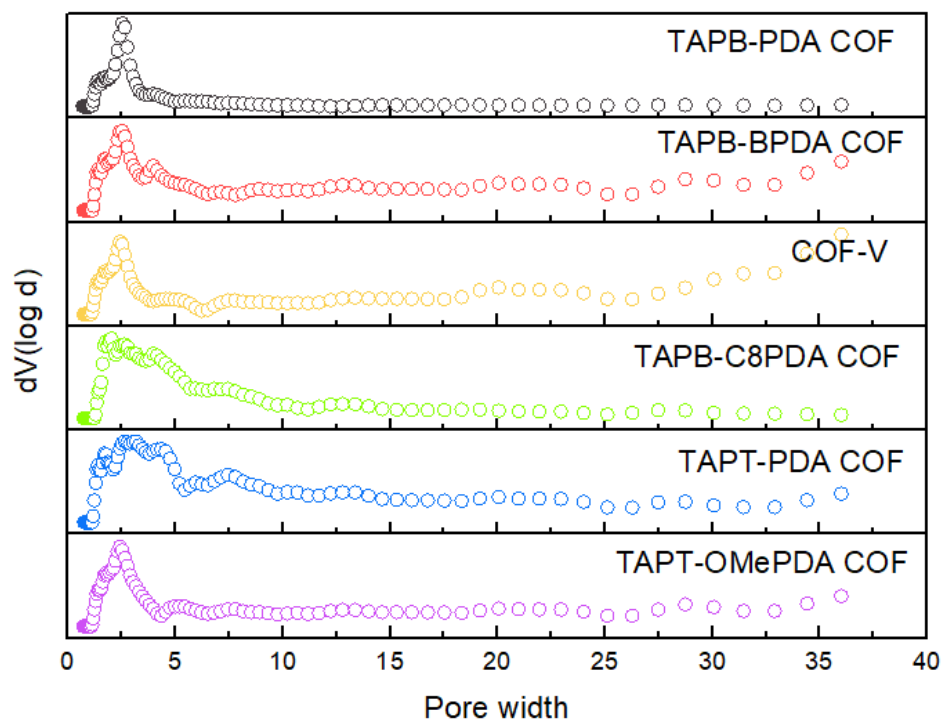


**Figure S31.** Pore size distributions of different COFs synthesized using 10mol% of Fe-NO for 2 hours

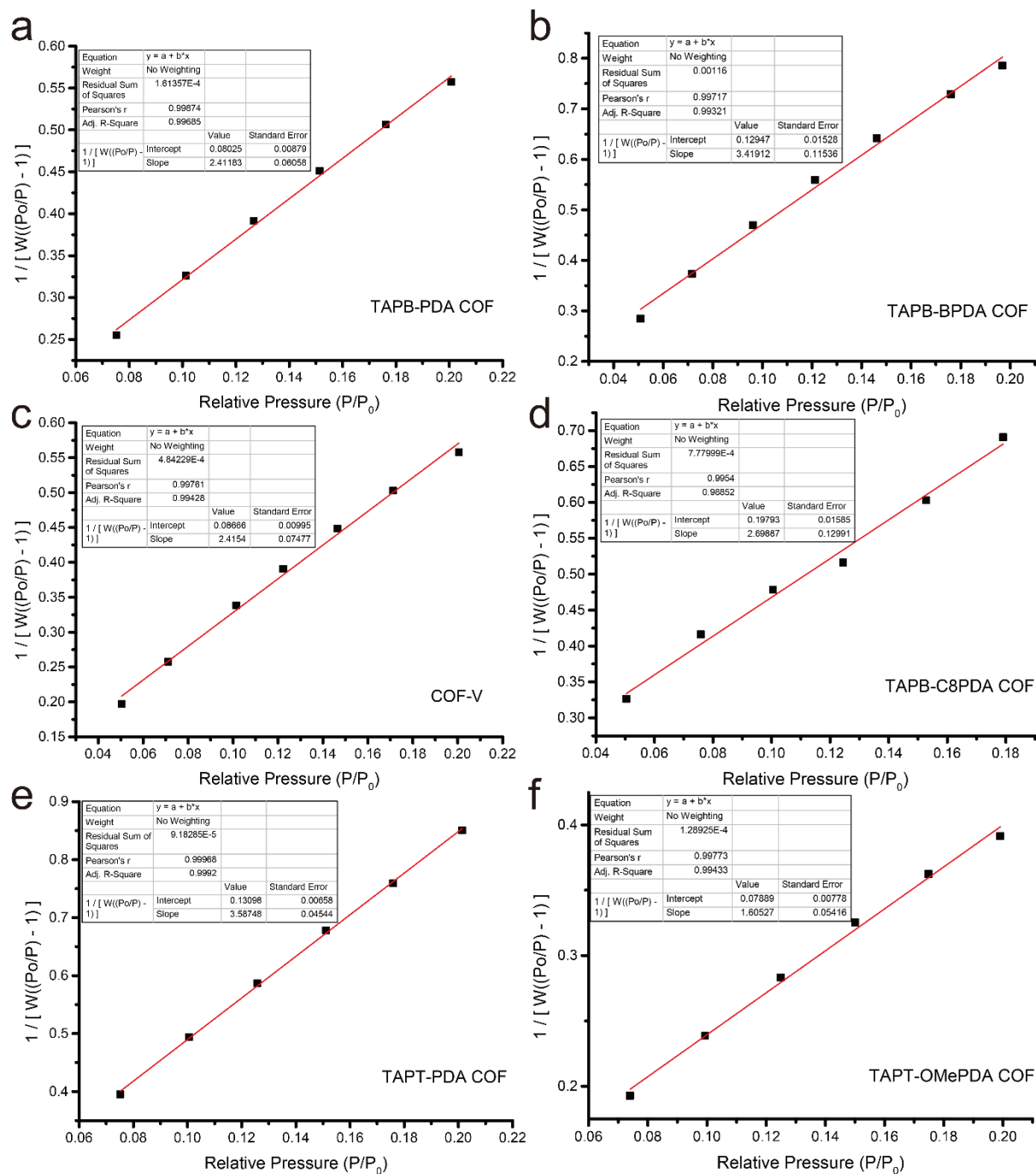


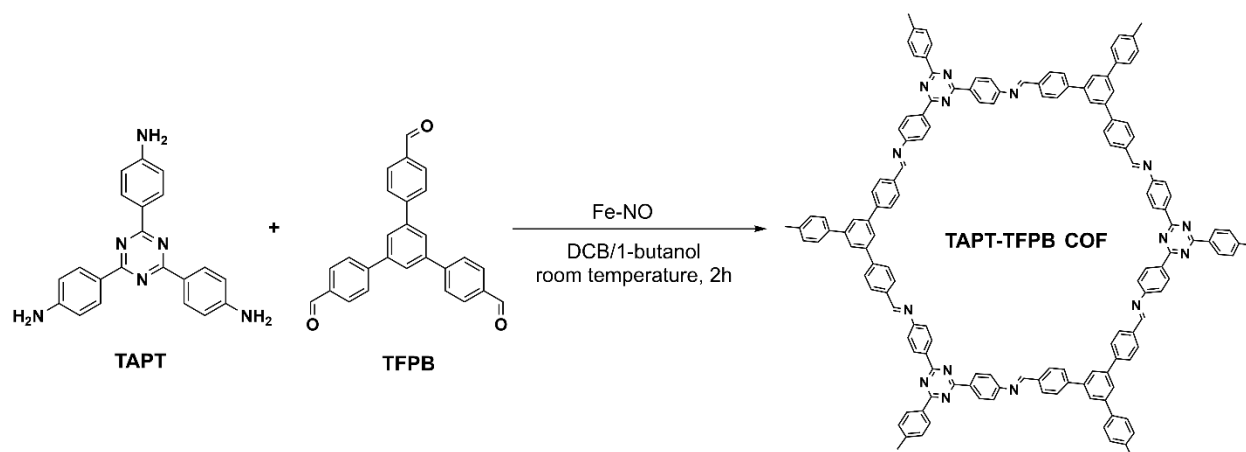
**Figure S32.** BET surface area calculations---t plot for different COFs synthesized using 10mol% of Fe-NO for 2 hours



**Table S3.** Summary of highest BET surface areas in previous work and comparison with our work

COF	S <sub>BET</sub> (m <sup>2</sup> g <sup>-1</sup> )	Synthesis conditions	reference
TAPB-PDA	2890	Solvothermal, 10.5 M acetic acid, dioxane/mesitylene (4:1, v/v), 70 °C, 4 h, ScCO <sub>2</sub>	Feriante, Cameron H., et al. <i>Advanced Materials</i> (2019): 1905776.
TAPB-PDA	1397	10 mol% Fe-NO, 1,2-dichlorobenzene/n-butyl alcohol (1:1, v/v), room temperature, 2 hours, ScCO <sub>2</sub> drying	Our work
TAPB-BPDA	1235	0.02 equivalent Sc(OTf) <sub>3</sub> , dioxane/mesitylene (4:1, v/v), room temperature, 30 minutes, ScCO <sub>2</sub> drying	Matsumoto, Michio, et al. <i>Journal of the American Chemical Society</i> 139.14 (2017): 4999-5002.
TAPB-BPDA	981	Same procedures as TAPB-PDA COF	Our work
COF-V	1152	Solvothermal, 6 M acetic acid, 1,2-dichlorobenzene/n-butyl alcohol (1:1, v/v), 100 °C, 3 days, THF Soxhlet for 2 days and vacuum activation at 50 °C	Sun, Qi, et al. <i>Journal of the American Chemical Society</i> 139.7 (2017): 2786-2793. Sun, Qi, et al. <i>Chem</i> 4.7 (2018): 1726-1739.
COF-V	1392	Same procedures as TAPB-PDA COF	Our work
TAPB-C8PDA (film)	29	<i>p</i> -toluenesulfonic acid (PTSA), acetonitrile/water interface, 3 days, washed with MeCN/H <sub>2</sub> O mixture, N,N-dimethylformamide, ethanol, and acetone, dried in oven under 60 °C for 12 h	Shao, Pengpeng, et al. <i>Angewandte Chemie International Edition</i> 57.50 (2018): 16501-16505.
TAPB-C8PDA	1202	Same procedures as TAPB-PDA COF	Our work
TAPT-PDA	716	DMF, reflux under N <sub>2</sub> gas for 12 hours, washed with DMF and ethanol, Soxhlet using methanol for 48 hours, did not mention drying	Gomes, Ruth, Piyali Bhanja, and Asim Bhaumik. <i>Chemical Communications</i> 51.49 (2015): 10050-10053.
TAPT-PDA	937	Same procedures as TAPB-PDA COF	Our work
TAPT-OMePDA	1305	Solvothermal, 3 M acetic acid, ethanol/1,2-dichlorobenzene (1:1, v/v), 120 °C, 3 days, THF vacuum activation	Mullangi, Dinesh, et al. <i>Small</i> 14.37 (2018): 1801233.
TAPT-OMePDA	2068	Same procedures as TAPB-PDA COF	Our work

### Synthesis of TAPT-TFPB COF through 3+3 node-linker construction strategy



**Scheme S7** Synthesis of TAPT-TFPB COF

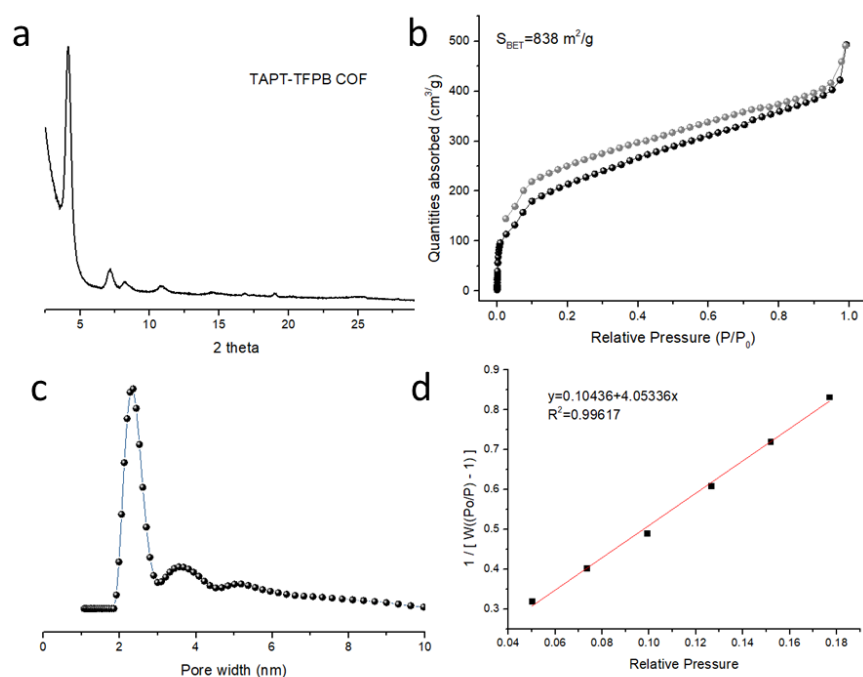


**Figure S33** (a) PXRD for TAPT-TFPB COF (b) nitrogen sorption of TAPT-TFPB COF (c) pore size distribution (d) t-plot to calculate the BET surface area

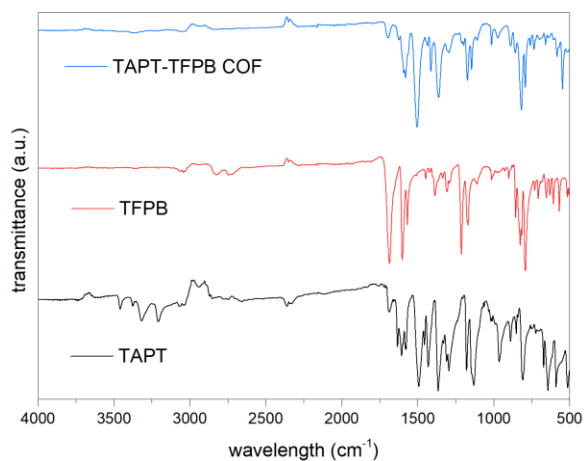
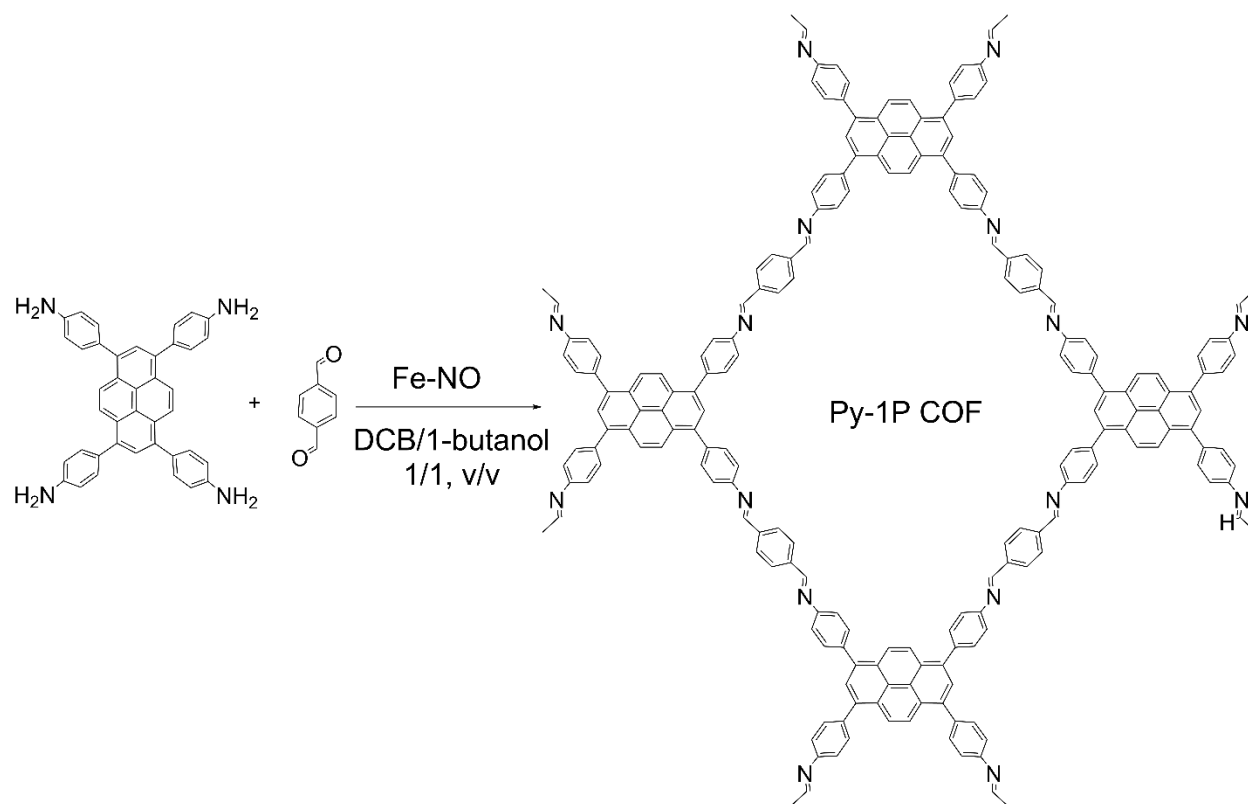


**Figure S34** (a) FTIR for TAPT amine monomer, TFPB aldehyde monomer and TAPT-TFPB COF

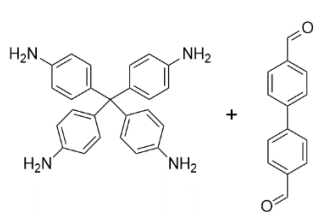
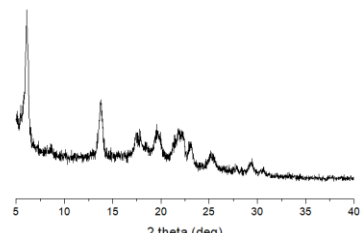
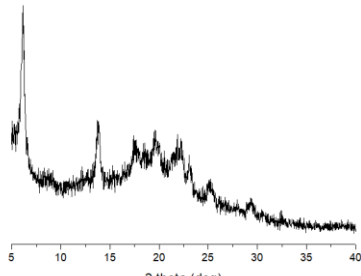
**Synthesis of Py-1P COF through 4+2 node-linker construction strategy**

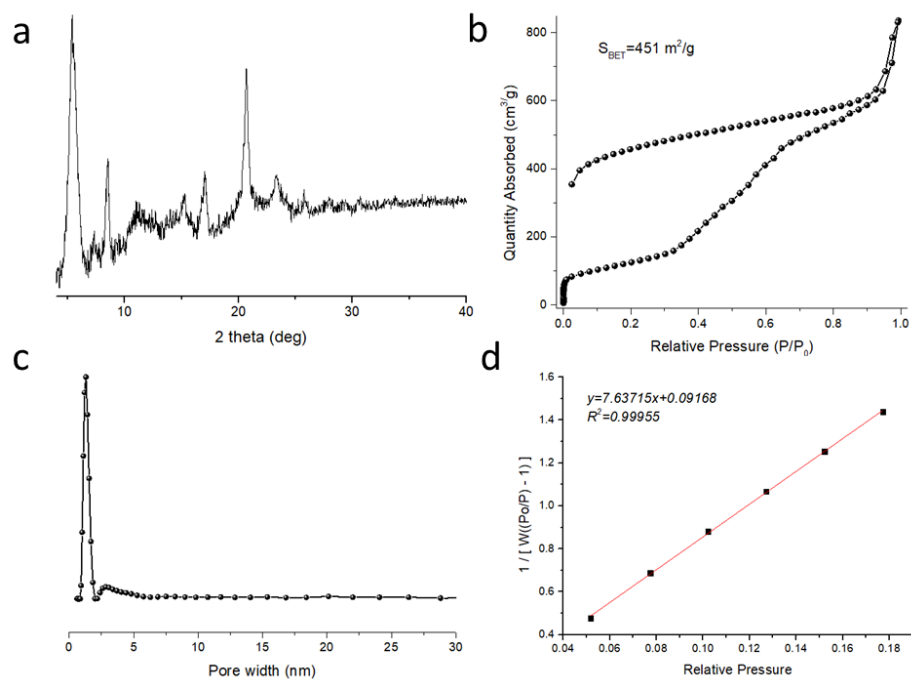


**Scheme S8** Synthesis of Py-1P COF

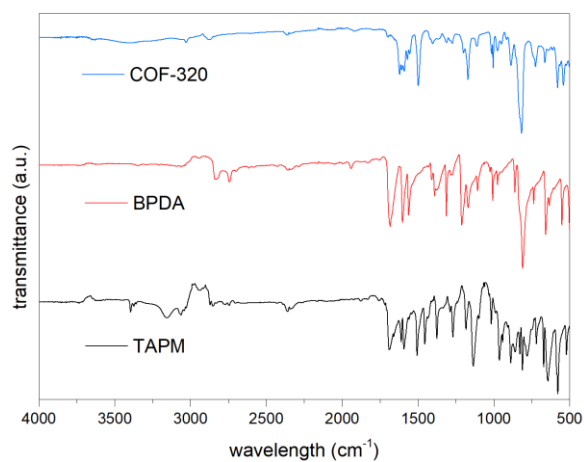
# Synthesis of 3D COF (COF320)

Table S4 synthesis conditions of COF-320

		
Cu-NO (10mol% of NH <sub>2</sub> )	DCB/1-butanol,1/1, v/v, room temperature, 4h	Crystalline, see Figure S35 a
Fe-NO (10mol% of NH <sub>2</sub> )	DCB/1-butanol,1/1, v/v, room temperature, 4h	no crystallinity
Ni-NO (10mol% of NH <sub>2</sub> )		
Zn-NO (10mol% of NH <sub>2</sub> )		
Co-NO (10mol% of NH <sub>2</sub> )		no crystallinity
Sc(OTf) <sub>3</sub> 1 mol%	DCB/1-butanol,1/1, v/v, room temperature, 4h	no crystallinity
Sc(OTf) <sub>3</sub> 1 mol%	Dioxane, room temperature, 4h	
6M acetic acid	DCB/1-butanol,1/1, v/v, room temperature, 4h	
6M acetic acid	Dioxane, room temperature, 4h	



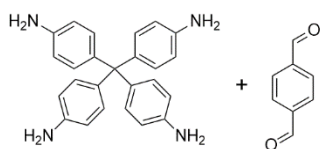
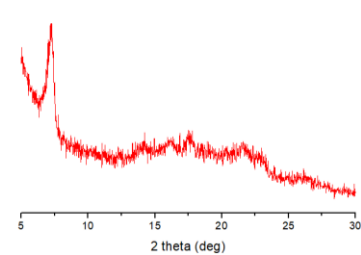
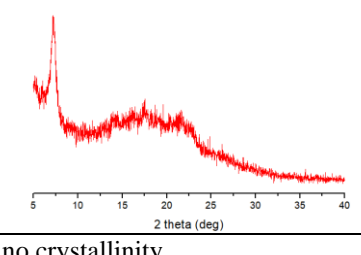
**Figure S35** (a) PXRD for COF-320 (b) nitrogen sorption of COF-320 (c) pore size distribution (d) t-plot to calculate the BET surface area



**Figure S36** (a) FTIR for TAPM amine monomer, BPDA aldehyde monomer and COF-320

# Synthesis of 3D COF (COF300)

**Table S5 synthesis conditions of COF-300**

		
Cu-NO (10mol% of NH <sub>2</sub> )	DCB/1-butanol,1/1, v/v, room temperature, 4h	Crystalline, Figure S37 a
Fe-NO (10mol% of NH <sub>2</sub> )	DCB/1-butanol,1/1, v/v, room temperature, 4h	no crystallinity
Ni-NO (10mol% of NH <sub>2</sub> )		
Zn-NO (10mol% of NH <sub>2</sub> )		
Co-NO (10mol% of NH <sub>2</sub> )		no crystallinity
Sc(OTf) <sub>3</sub> 1 mol%	DCB/1-butanol,1/1, v/v, room temperature, 4h	no crystallinity
Sc(OTf) <sub>3</sub> 1 mol%	Dioxane, room temperature, 4h	
6M acetic acid	DCB/1-butanol,1/1, v/v, room temperature, 4h	
6M acetic acid	Dioxane, room temperature, 4h	

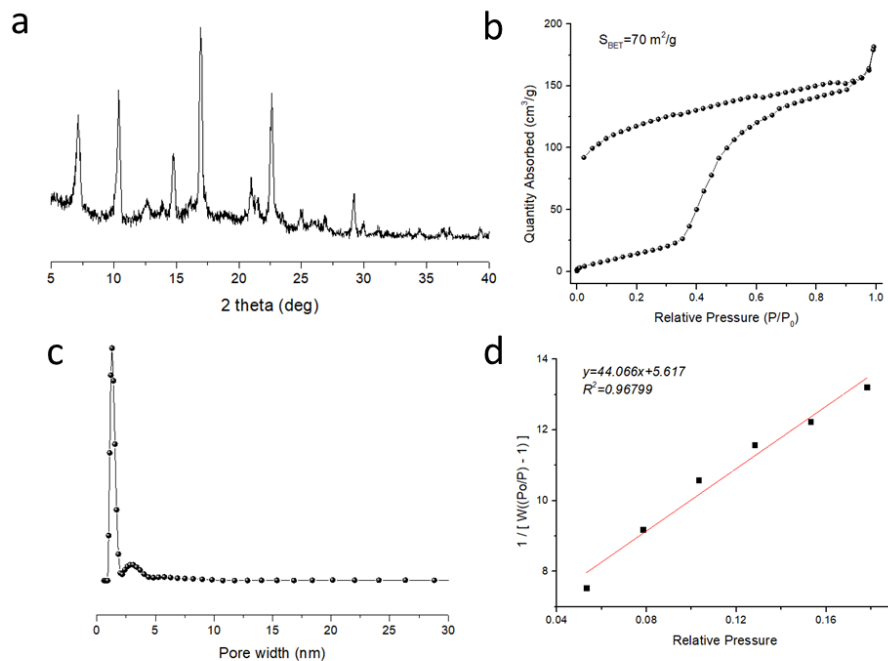


**Figure S37** (a) PXRD for COF-300 (b) nitrogen sorption of COF-300 (c) pore size distribution (d) t-plot to calculate the BET surface area

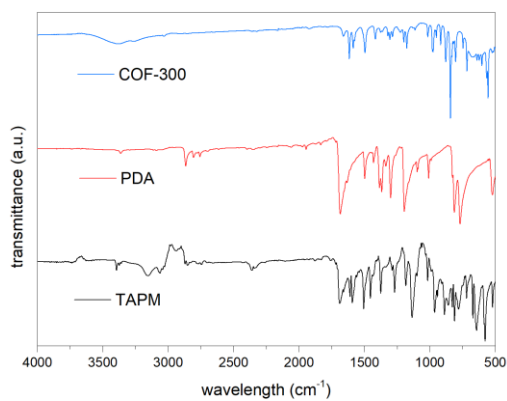
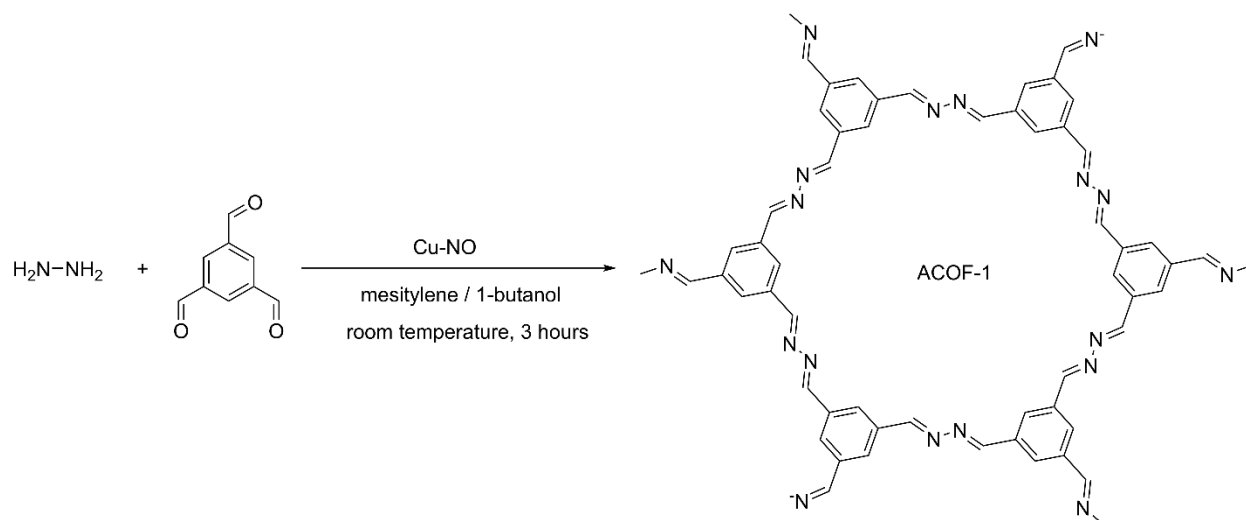


**Figure S38** (a) FTIR for TAPM amine monomer, PDA aldehyde monomer and COF-300

## Synthesis of azine-linked COF



**Scheme S9** Synthesis of azine-linked COF (ACOF-1)

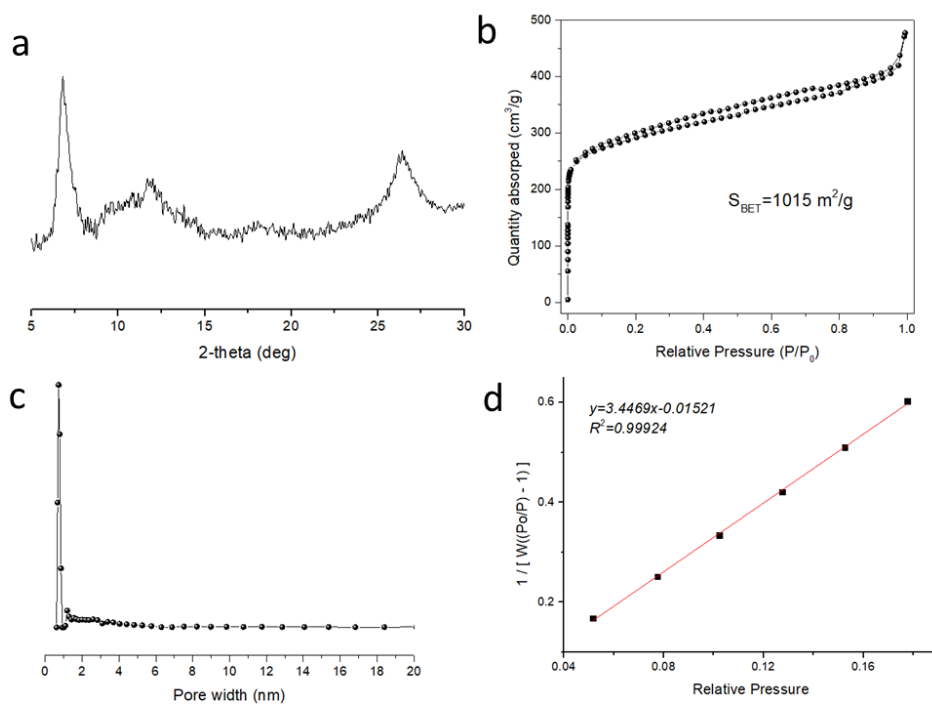


**Figure S39** (a) PXRD for ACOF-1 (b) nitrogen sorption of ACOF-1 (c) pore size distribution (d) t-plot to calculate the BET surface area



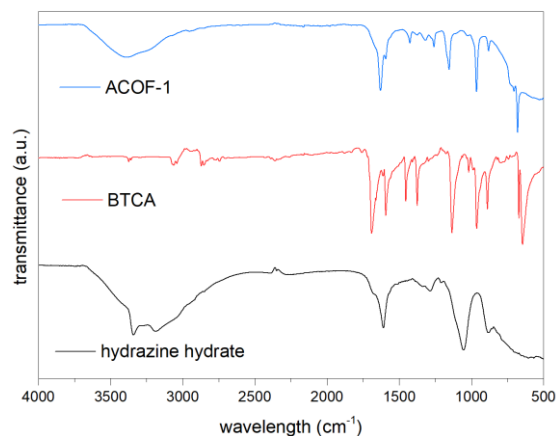


**Figure S40** (a) FTIR for hydrazine monohydrate monomer, BTCA aldehyde monomer and ACOF-1

### Synthesis of $\beta$ -ketoenamine COF

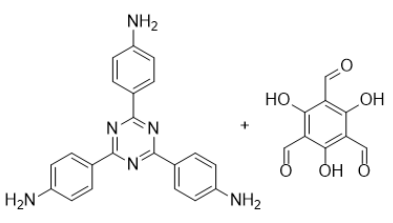
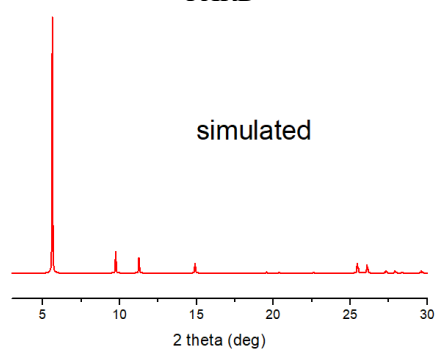
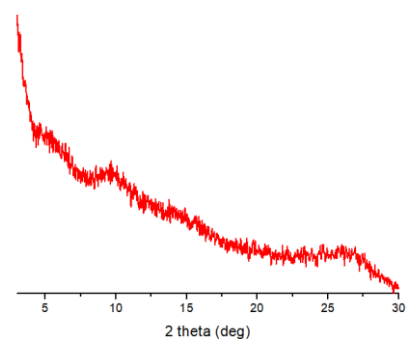
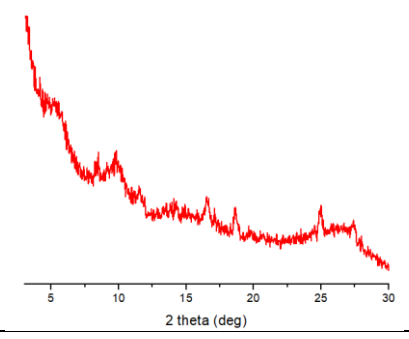
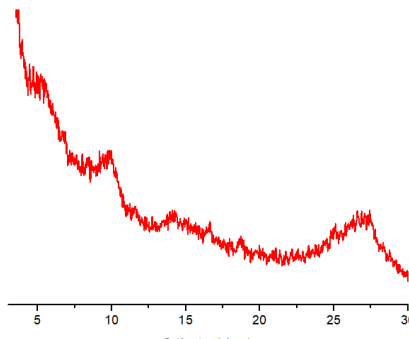

We tested the synthesize  $\beta$ -ketoenamine COFs, but only obtained products with limited crystallinity. However, we could produce  $\beta$ -ketoenamine COFs with higher crystallinity at elevated temperature (120 °C), indicating metal nitrates may have the potential in catalyzing  $\beta$ -ketoenamine COFs.  $\beta$ -ketoenamine COFs themselves are difficult to be synthesized with high crystallinity and porosity even under solvothermal conditions due to the irreversible tautomerism from imine to ketone. The BET surface areas of some reported  $\beta$ -ketoenamine COFs are listed in Table S6.

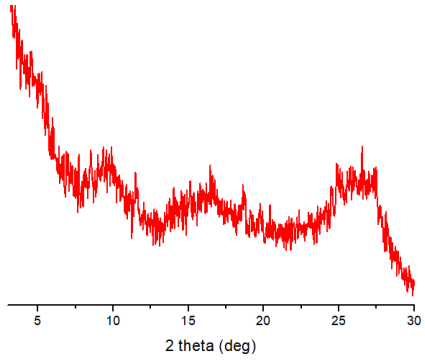
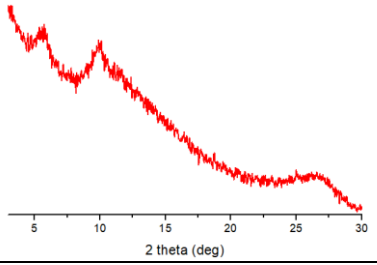
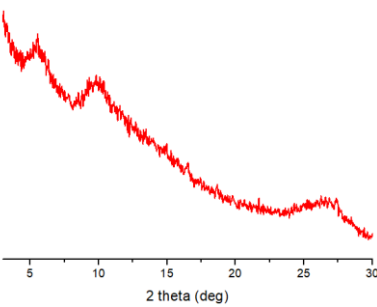
The synthesis conditions tested and corresponding PXRD data are provided in Table S7. We also tried to use  $\text{Sc}(\text{OTf})_3$  and 6M acetic acid to synthesize this COF within 6 hours at room temperature, but no crystallinity was observed.

**Table S6** BET surface areas of  $\beta$ -ketoenamine COFs from previous reports

COF name	BET surface areas( $\text{m}^2/\text{g}$ )	reference
DAAQ-TFP COF	435	<i>J. Am. Chem. Soc.</i> 2013, 135, 45, 16821–16824
DAB-TFP COF	365	<i>J. Am. Chem. Soc.</i> 2013, 135, 45, 16821–16824
TFP-TPA	457	<i>Journal of the Taiwan Institute of Chemical Engineers</i> , 2019, 103: 199-208.
TFP-Car	362	<i>Journal of the Taiwan Institute of Chemical Engineers</i> , 2019, 103: 199-208.
TpPa-2	339	<i>J. Am. Chem. Soc.</i> 2012, 134, 48, 19524–19527

**Table S7 Synthesis conditions of  $\beta$ -ketoenamine TAPT-TFP COFs and their PXRD results**

		<p>PXRD</p>  <p>simulated</p>
Fe-NO (10mol% of NH <sub>2</sub> )	mesitylene/1-butanol, room temperature, 6h	
Ni-NO (10mol% of NH <sub>2</sub> )		
Cu-NO (10mol% of NH <sub>2</sub> )		
Zn-NO (10mol% of NH <sub>2</sub> )		

		 <p>5 10 15 20 25 30</p> <p>2 theta (deg)</p>
Fe-NO (10mol% of NH <sub>2</sub> )	mesitylene/1-butanol, 120 °C, 6h	 <p>5 10 15 20 25 30</p> <p>2 theta (deg)</p>
Cu-NO (10mol% of NH <sub>2</sub> )		 <p>5 10 15 20 25 30</p> <p>2 theta (deg)</p>

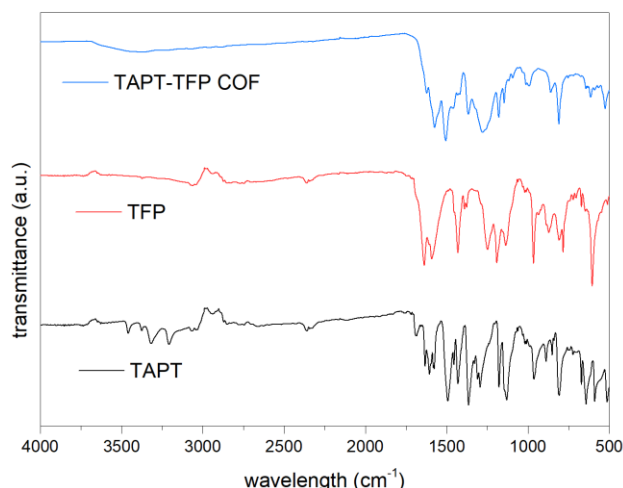


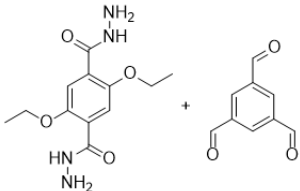
**Figure S41** (a) FTIR for TAPT monomer, TFP aldehyde monomer and  $\beta$ -ketoenamine-linked TAPT-TFP COF

### Synthesis of hydrazone COF

We tested the synthesis hydrazone COFs using the conditions listed in Table S8, but these tests were unsuccessful. Possible reasons are that hydrazide monomer has poor solubility at room temperature, and the reactivity of hydrazine monomer is much lower than amine monomer. We also tried to use  $\text{Sc}(\text{OTf})_3$  and 6M acetic acid to synthesize hydrazone COFs at room temperature within 2 hours, and no crystalline samples could be obtained.

Not many hydrazone-linked COFs have been designed and synthesized due to the limited monomer types. Instead, imine-COFs are most widely investigated and the importance of imine-COFs are much higher than hydrazone COFs. So, we believe that metal nitrates are still very important even though they lack the efficiency to catalyze hydrazone COFs.

**Table S8** Synthesis conditions of hydrazone COFs

		
Fe-NO (10mol% of $\text{NH}_2$ )	DCB/1-butanol, 1/1, v/v, room temperature, 2h	no crystallinity
Ni-NO (10mol% of $\text{NH}_2$ )		
Cu-NO (10mol% of $\text{NH}_2$ )		
Zn-NO (10mol% of $\text{NH}_2$ )		
Co-NO (10mol% of $\text{NH}_2$ )		
$\text{Sc}(\text{OTf})_3$ 1 mol%	DCB/1-butanol, 1/1, v/v, room temperature, 2h	
$\text{Sc}(\text{OTf})_3$ 1 mol%	dioxane/mesitylene, 1/3, v/v, room temperature, 2h	
6M acetic acid	DCB/1-butanol, 1/1, v/v, room temperature, 2h	
6M acetic acid	dioxane/mesitylene, 1/3, v/v, room temperature, 2h	

## **$^1\text{H}$ - $^{13}\text{C}$ cross polarization, magic angle spinning (CPMAS) NMR study**

TAPB-OMePDA COF samples obtained using Fe-NO catalysts were analyzed using  $^1\text{H}$ - $^{13}\text{C}$  cross polarization, magic angle spinning (CPMAS) NMR.

The centerband region of the  $^1\text{H}$ - $^{13}\text{C}$  CPMAS spectra of TAPB-OMePDA COF obtained with 15 different contact times is shown in Figures S42-S56. The 15 spectra are plotted with the same level of baseline noise to facilitate comparison. There is no contact time at which accurate relative signal intensities are obtained because the signals cross polarize at significantly different rates.

The centerband region of the standard CPMAS spectra obtained with a contact time of 3.0 ms and with dipolar dephasing intervals of 50  $\mu\text{s}$  and 80  $\mu\text{s}$  is shown in Figure S57. These three spectra are plotted with the same level of baseline noise to facilitate comparison. A highly expanded plot of the methoxy carbon signal in the standard CPMAS spectrum obtained with a contact time of 3.0 ms is shown in Figure S58. This signal is not a symmetric single peak; it is a collection of overlapping signals with slightly different chemical shifts. The same asymmetry is evident in a previously reported spectrum of this COF.<sup>1</sup> Slightly different methoxy environments can be expected at the edges of the COF. The distinctive methoxy carbon chemical shift enables the detection of the slightly different environments.

$^{13}\text{C}$  chemical shift assignments for the precursors TAPB and OMePDA dissolved in DMSO- $d_6$  enabled a more secure analysis of the signals in the CPMAS spectra of TAPB-OMePDA COF. Assignments for TAPB resulted from a combination of  $^1\text{H}$ ,  $^{13}\text{C}$ , DEPT-135  $^{13}\text{C}$ , HSQC, and HMBC spectra:  $\delta$ 148.38 (amino-substituted carbon),  $\delta$ 141.61 (quaternary carbon of trisubstituted ring),  $\delta$ 128.06 (quaternary carbon next to trisubstituted ring),  $\delta$ 127.48 (aromatic CH *meta* to amino group),  $\delta$ 120.40 (aromatic CH of trisubstituted ring),  $\delta$ 114.21 (aromatic CH *ortho* to amino group). Assignments for OMePDA resulted from a combination of  $^1\text{H}$ ,  $^{13}\text{C}$ , and DEPT-135  $^{13}\text{C}$  spectra:  $\delta$ 189.08 (carbonyl),  $\delta$ 155.24 (methoxy-substituted aromatic carbon),  $\delta$ 128.78 (aldehyde-substituted aromatic carbon),  $\delta$ 111.30 (aromatic CH),  $\delta$ 56.46 (methoxy).

In TAPB-OMePDA COF, the relatively fast buildup of the signals (as the contact time is lengthened) at about 155.8 and 150.4 ppm (in the spectrum with  $t_{\text{cp}} = 0.10$  ms) is consistent with the imino -CH=N- group. The much slower build up of the signals at about 153.1 and 148.0 ppm (in the spectrum with  $t_{\text{cp}} = 0.10$  ms) is consistent with the aromatic carbon bonded to methoxy. This conclusion is reinforced by comparing the standard cross polarization spectrum obtained with  $t_{\text{cp}} = 3.0$  ms, the cross polarization spectrum obtained with  $t_{\text{cp}} = 3.0$  ms and a dipolar dephasing delay of 50  $\mu\text{s}$ , and the cross polarization spectrum obtained with  $t_{\text{cp}} = 3.0$  ms and a dipolar dephasing delay of 80  $\mu\text{s}$  (Figure S57). The very unequal intensities of the signals at 153.1 and 148.0 ppm at longer contact times are consistent with the stronger signal (153.1 ppm) also resulting from the quaternary aromatic carbon bonded to the imino nitrogen. This carbon gives a signal at 152.2 ppm in the model compound N-benzylideneaniline ( $\text{C}_6\text{H}_5\text{-CH=N-C}_6\text{H}_5$ ).<sup>2</sup>

The overlapping signals at 139.8 and 136.7 ppm cross polarize relatively slowly and dephase relatively slowly. They clearly are quaternary aromatic carbons. The chemical shifts suggest the quaternary aromatic carbon *of* the trisubstituted ring.

The strong signal at 126.9 ppm results from aromatic CH and quaternary aromatic carbon (a significant signal remains in the dipolar dephasing spectra). The chemical shift suggests the quaternary carbon *bonded to* the trisubstituted ring.

The quaternary aromatic carbon bonded to the imino =CH may be contributing to the intensity at 139.8 and 136.7 ppm. This carbon gives a signal at 136.4 ppm in the model compound N-benzylideneaniline ( $\text{C}_6\text{H}_5\text{-CH=N-C}_6\text{H}_5$ ).<sup>2</sup>

The signal at 121.3 ppm cross polarizes relatively quickly and dephases relatively quickly. The chemical shift suggests the aromatic CH of the trisubstituted ring.

The aromatic CH *meta* to the imino group probably contributes to the signal at 126.9 ppm.

The aromatic signals upfield of 120 ppm are relatively shielded. All are CH because they cross polarize relatively quickly and dephase relatively quickly. They most likely are CH adjacent to methoxy and *ortho* to imino.

The CPMAS spectra obtained at the various contact times show significantly more detail than the CPMAS spectra of the same COF reported by Li *et al.*<sup>1</sup> and Shao *et al.*<sup>3</sup> In all cases, the aldehyde carbon signal is extremely weak or undetectable, consistent with extensive condensation of amino and aldehyde functional groups to form imino groups. Our assignments differ from some of those by Shao *et al.*<sup>3</sup>—specifically, the aromatic C-O, the aromatic CH of the trisubstituted ring, and the quaternary aromatic carbon of the trisubstituted ring.

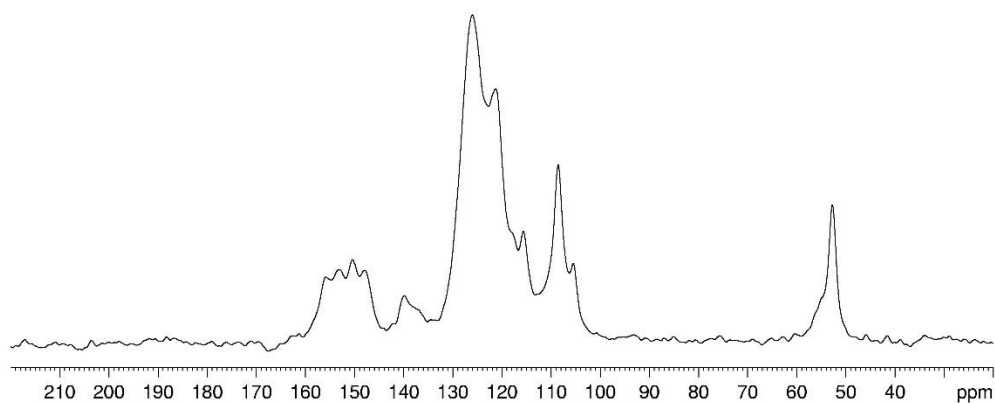


Figure S42. Centerband region of  $^1\text{H}$ - $^{13}\text{C}$  CPMAS spectrum ( $t_{\text{cp}} = 0.10$  ms) of TAPB-OMePDA COF

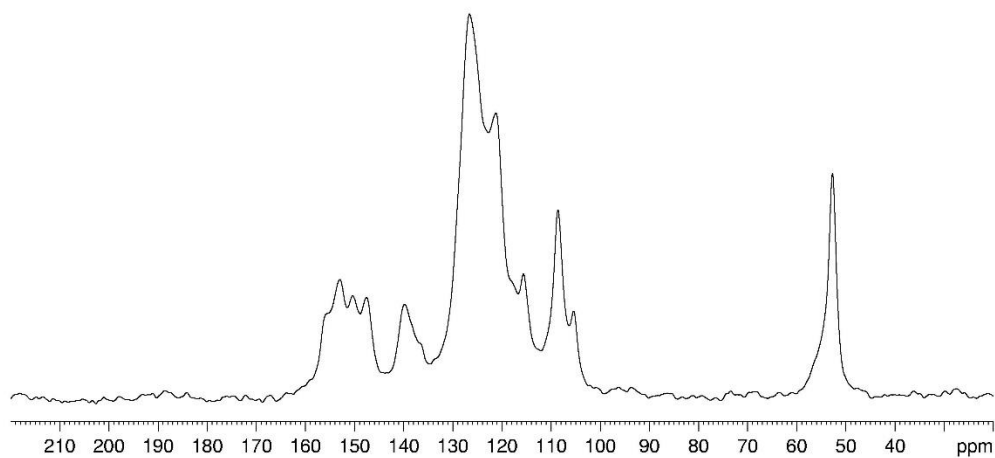


Figure S43. Centerband region of  $^1\text{H}$ - $^{13}\text{C}$  CPMAS spectrum ( $t_{\text{cp}} = 0.20$  ms) of TAPB-OMePDA COF

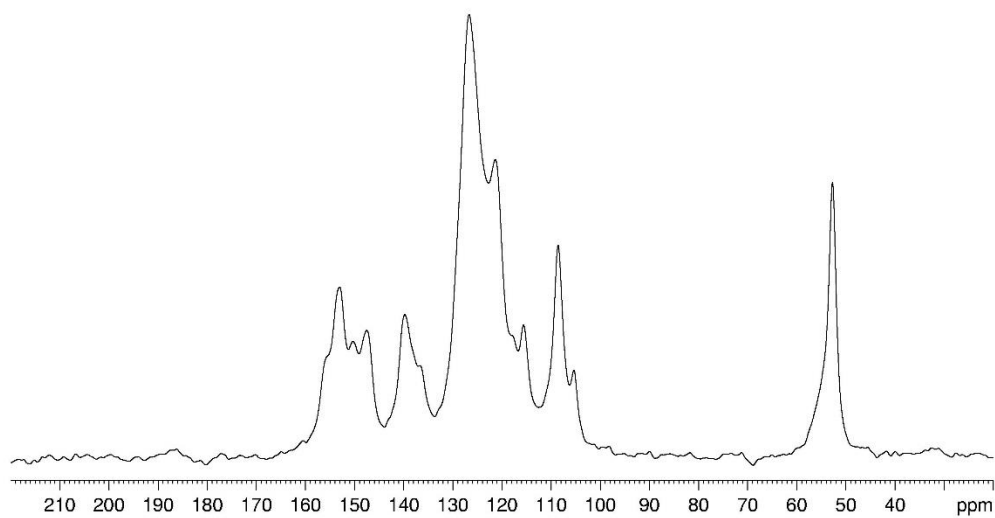


Figure S44. Centerband region of  $^1\text{H}$ - $^{13}\text{C}$  CPMAS spectrum ( $t_{\text{cp}} = 0.35$  ms) of TAPB-OMePDA COF

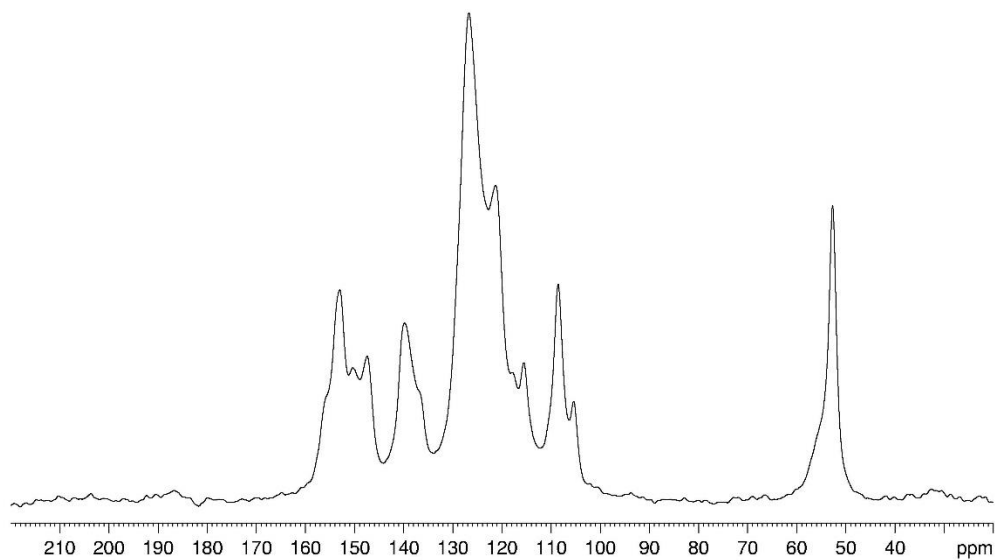


Figure S45. Centerband region of  ${}^1\text{H}$ - ${}^{13}\text{C}$  CPMAS spectrum ( $t_{\text{cp}} = 0.50$  ms) of TAPB-OMePDA COF

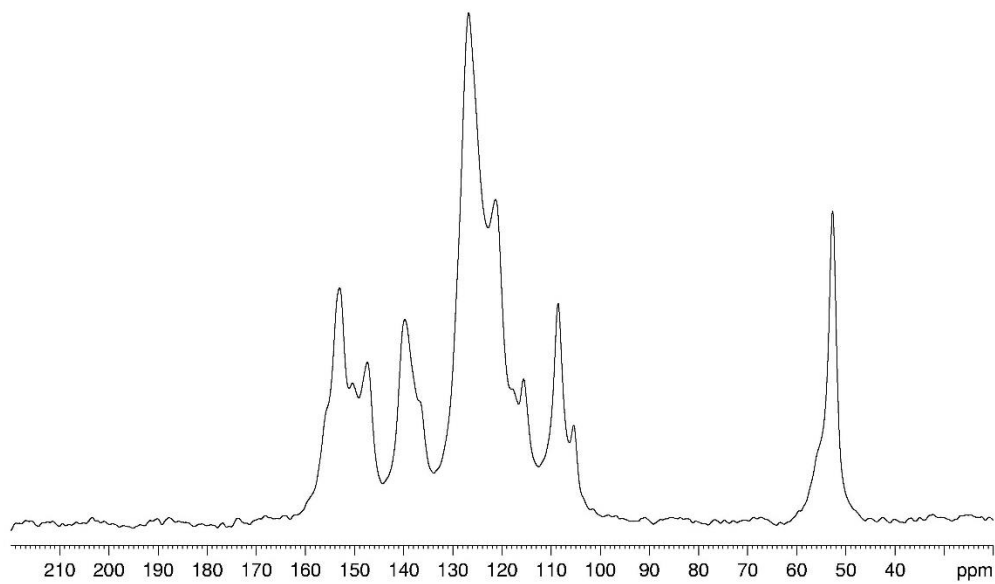


Figure S46. Centerband region of  ${}^1\text{H}$ - ${}^{13}\text{C}$  CPMAS spectrum ( $t_{\text{cp}} = 0.65$  ms) of TAPB-OMePDA COF



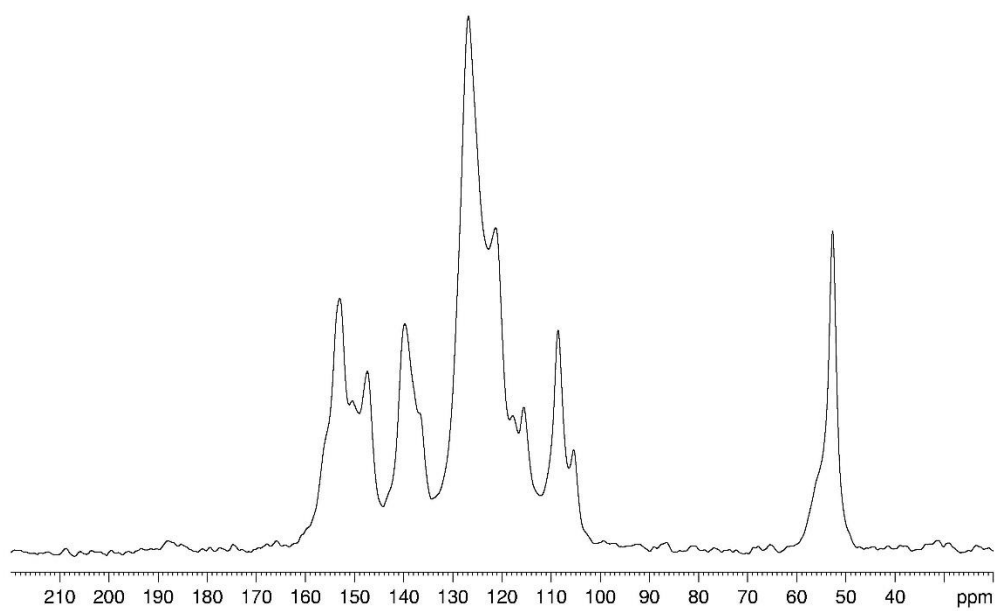


Figure S47. Centerband region of  $^1\text{H}$ - $^{13}\text{C}$  CPMAS spectrum ( $t_{\text{cp}} = 0.80$  ms) of TAPB-OMePDA COF

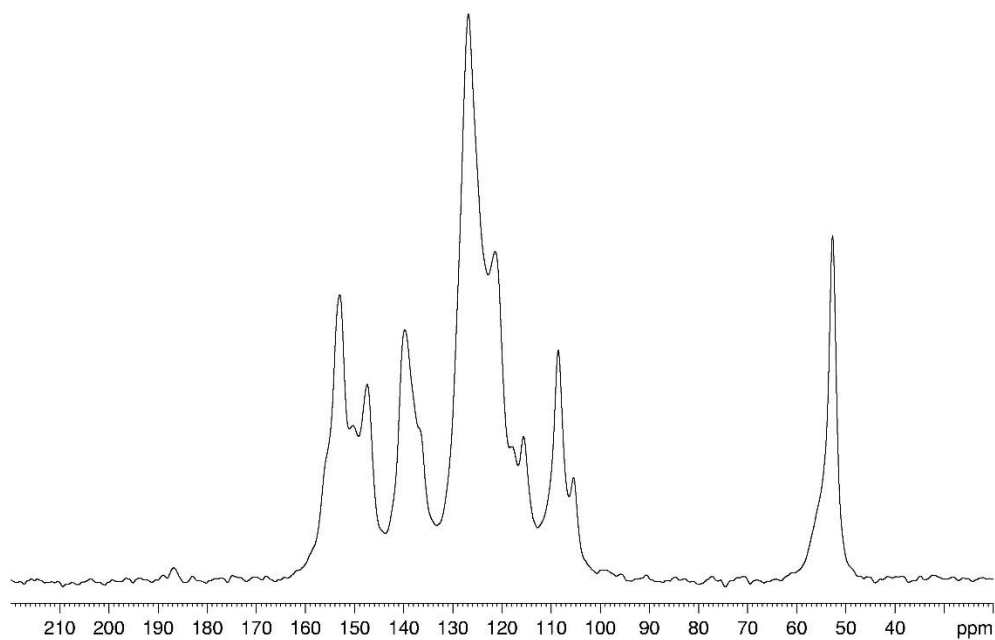


Figure S48. Centerband region of  $^1\text{H}$ - $^{13}\text{C}$  CPMAS spectrum ( $t_{\text{cp}} = 1.0$  ms) of TAPB-OMePDA COF

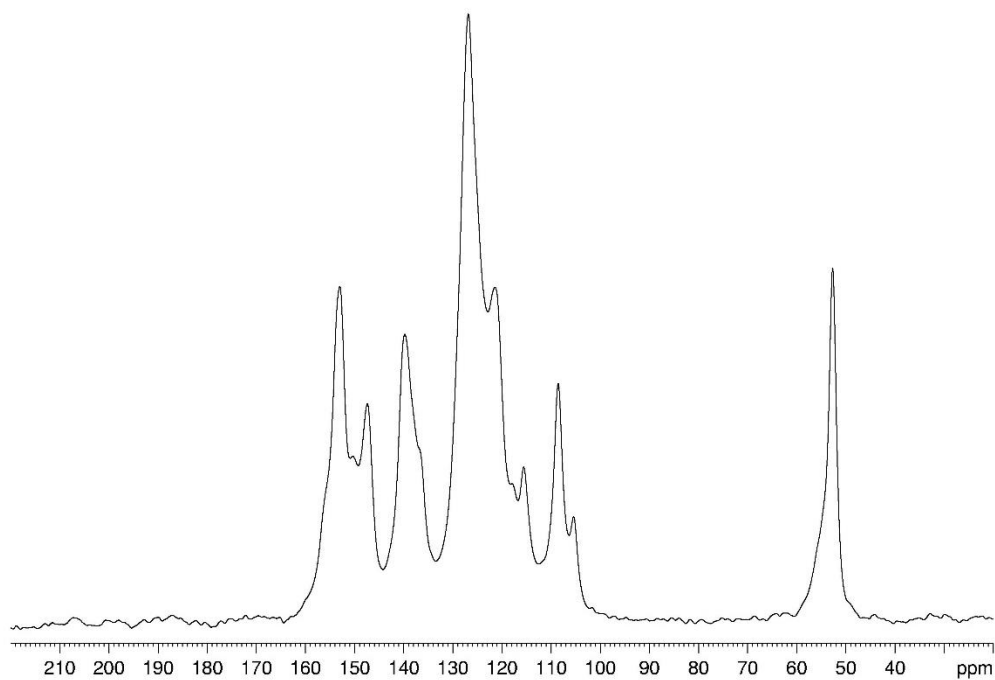


Figure S49. Centerband region of  $^1\text{H}$ - $^{13}\text{C}$  CPMAS spectrum ( $t_{\text{cp}} = 1.3$  ms) of TAPB-OMePDA COF

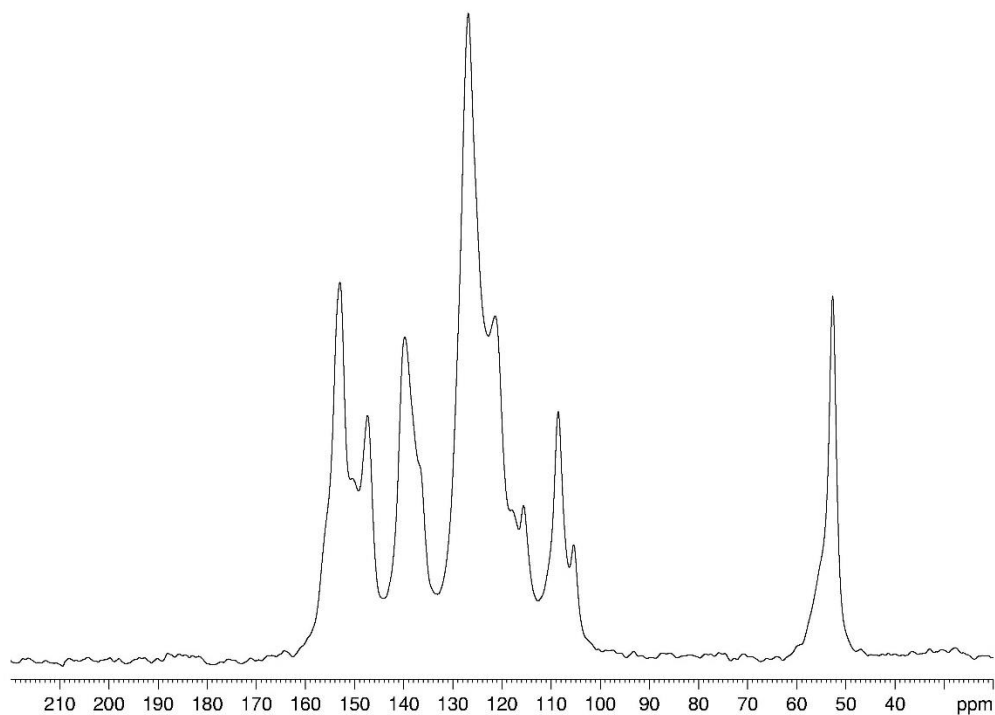


Figure S50. Centerband region of  $^1\text{H}$ - $^{13}\text{C}$  CPMAS spectrum ( $t_{\text{cp}} = 1.6$  ms) of TAPB-OMePDA COF

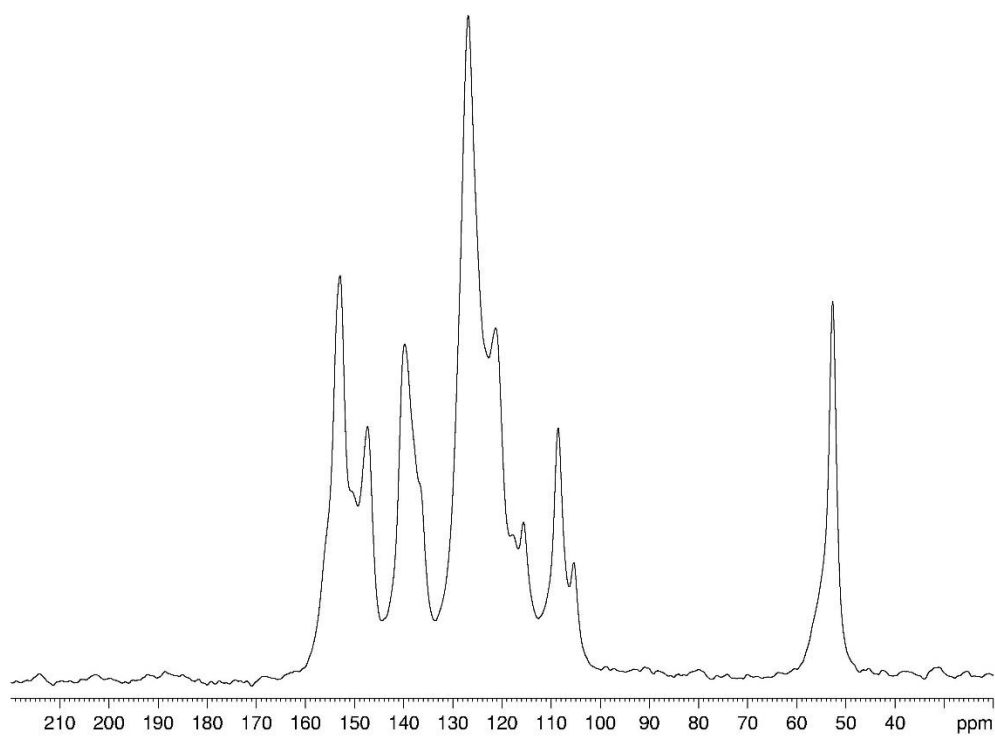


Figure S51. Centerband region of  $^1\text{H}$ - $^{13}\text{C}$  CPMAS spectrum ( $t_{\text{cp}} = 2.0$  ms) of TAPB-OMePDA COF

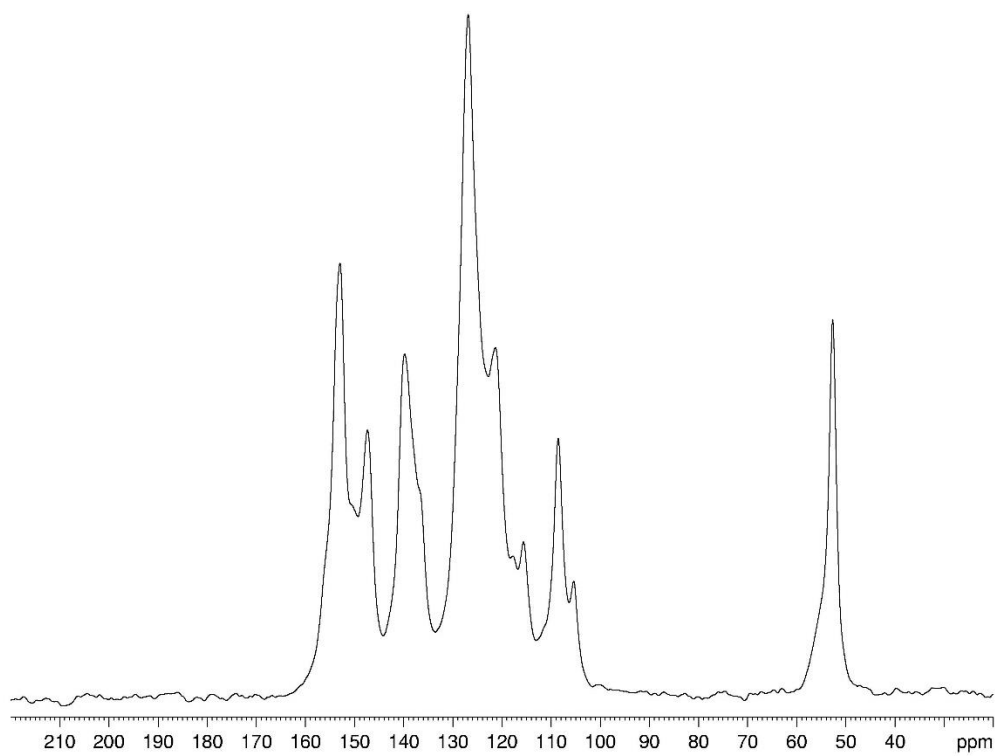


Figure S52. Centerband region of  $^1\text{H}$ - $^{13}\text{C}$  CPMAS spectrum ( $t_{\text{cp}} = 2.5$  ms) of TAPB-OMePDA COF

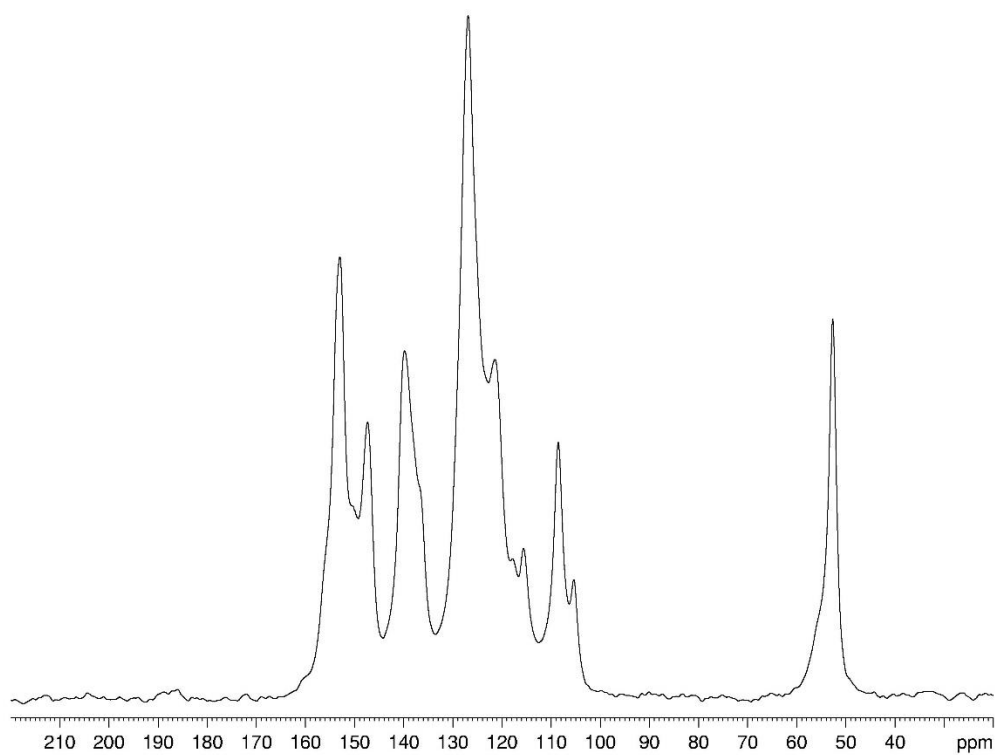


Figure S53. Centerband region of  $^1\text{H}$ - $^{13}\text{C}$  CPMAS spectrum ( $t_{\text{cp}} = 3.0$  ms) of TAPB-OMePDA COF

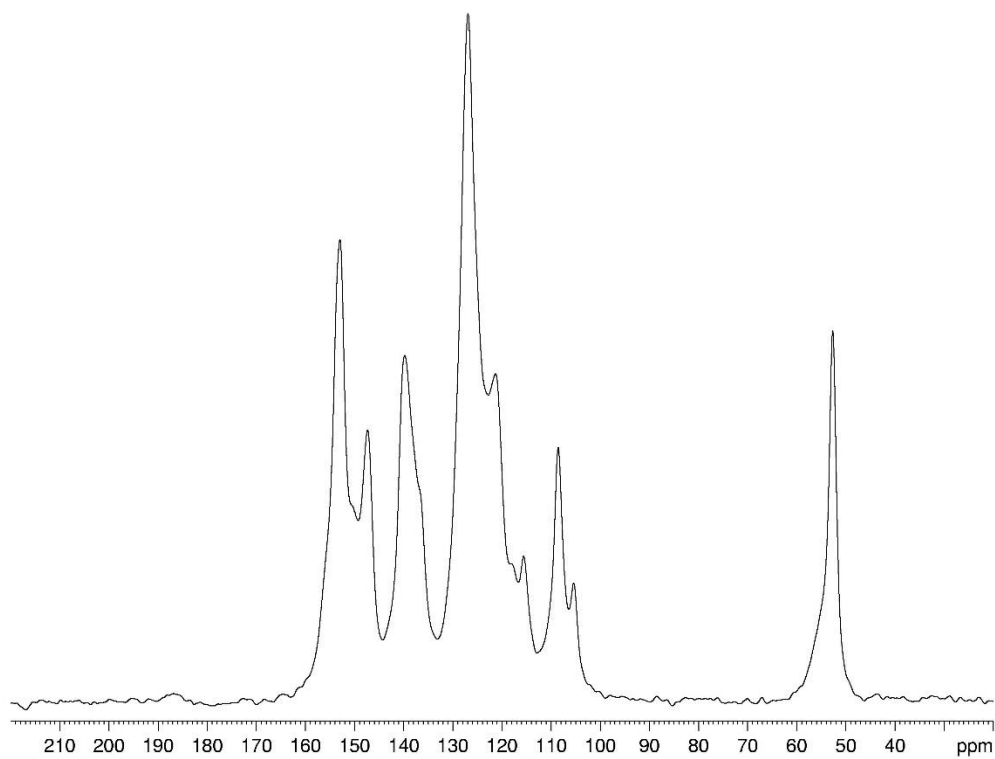


Figure S54. Centerband region of  $^1\text{H}$ - $^{13}\text{C}$  CPMAS spectrum ( $t_{\text{cp}} = 3.75$  ms) of TAPB-OMePDA COF

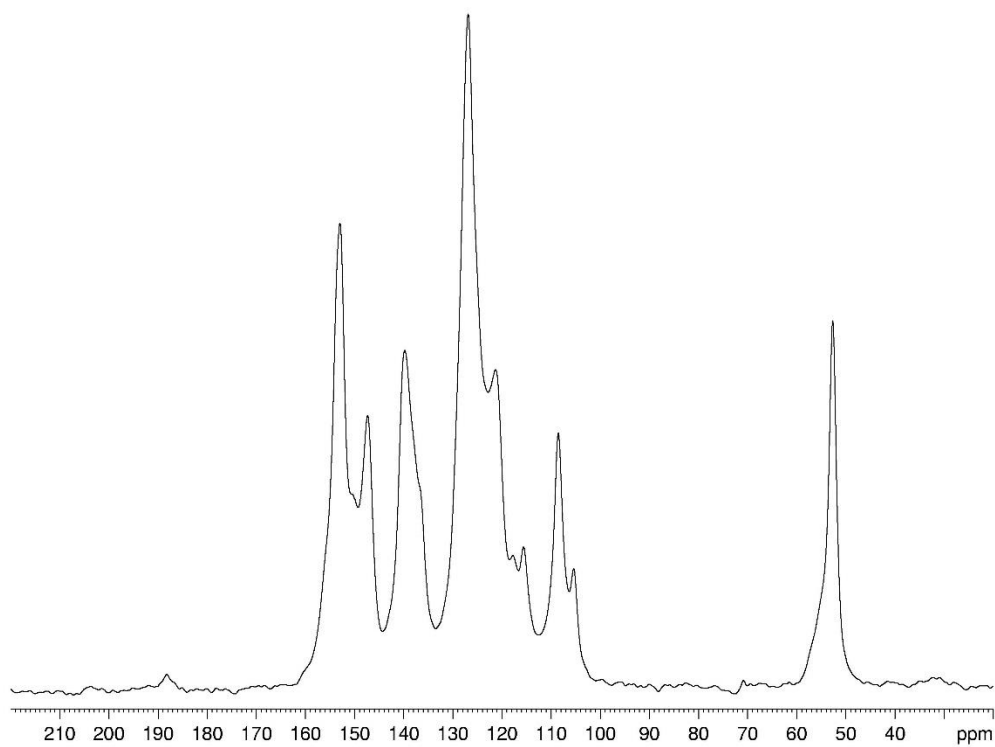


Figure S55. Centerband region of  $^1\text{H}$ - $^{13}\text{C}$  CPMAS spectrum ( $t_{\text{cp}} = 4.5$  ms) of TAPB-OMePDA COF

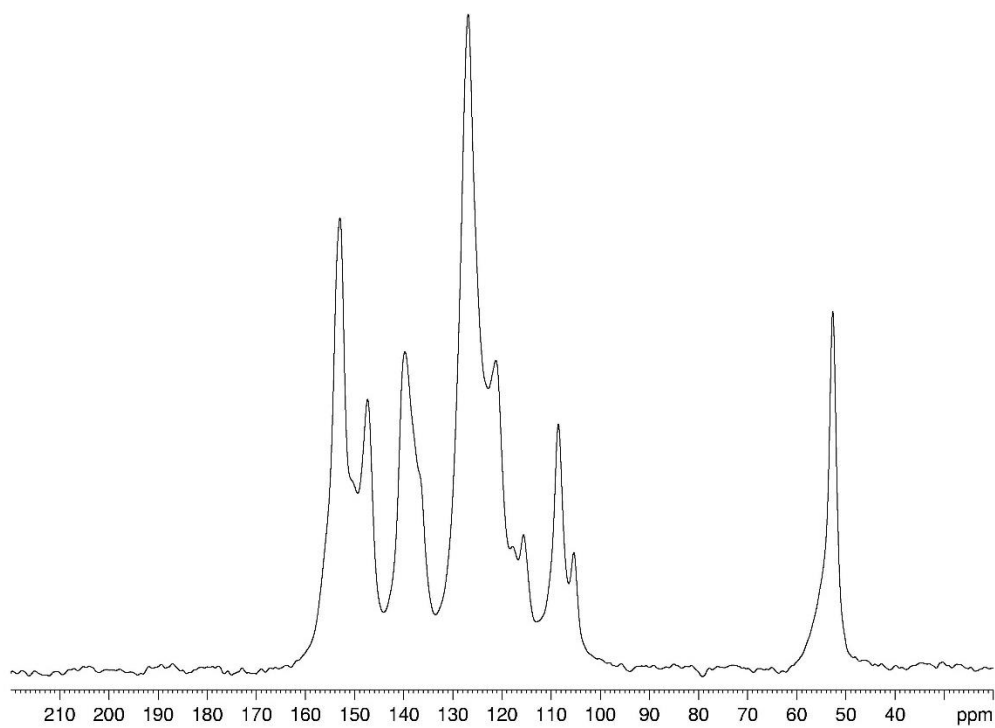


Figure S56. Centerband region of  $^1\text{H}$ - $^{13}\text{C}$  CPMAS spectrum ( $t_{\text{cp}} = 5.5$  ms) of TAPB-OMePDA COF

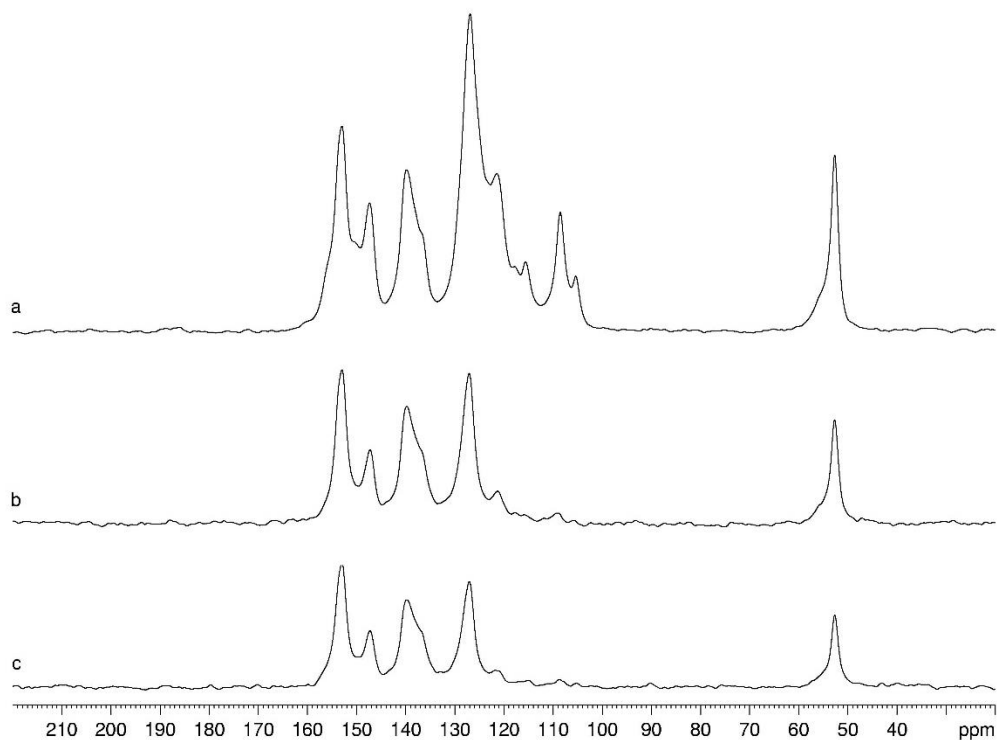


Figure S57. Centerband region of (a)  $^1\text{H}$ - $^{13}\text{C}$  CPMAS spectrum ( $t_{\text{cp}} = 3.0$  ms) of TAPB-OMePDA COF, (b)  $^1\text{H}$ - $^{13}\text{C}$  CPMAS spectrum ( $t_{\text{cp}} = 3.0$  ms) of TAPB-OMePDA COF with a 50- $\mu\text{s}$  dephasing interval, (c)  $^1\text{H}$ - $^{13}\text{C}$  CPMAS spectrum ( $t_{\text{cp}} = 3.0$  ms) of TAPB-OMePDA COF with a 80- $\mu\text{s}$  dephasing interval. Spectra are plotted with the same level of baseline noise to facilitate comparison.

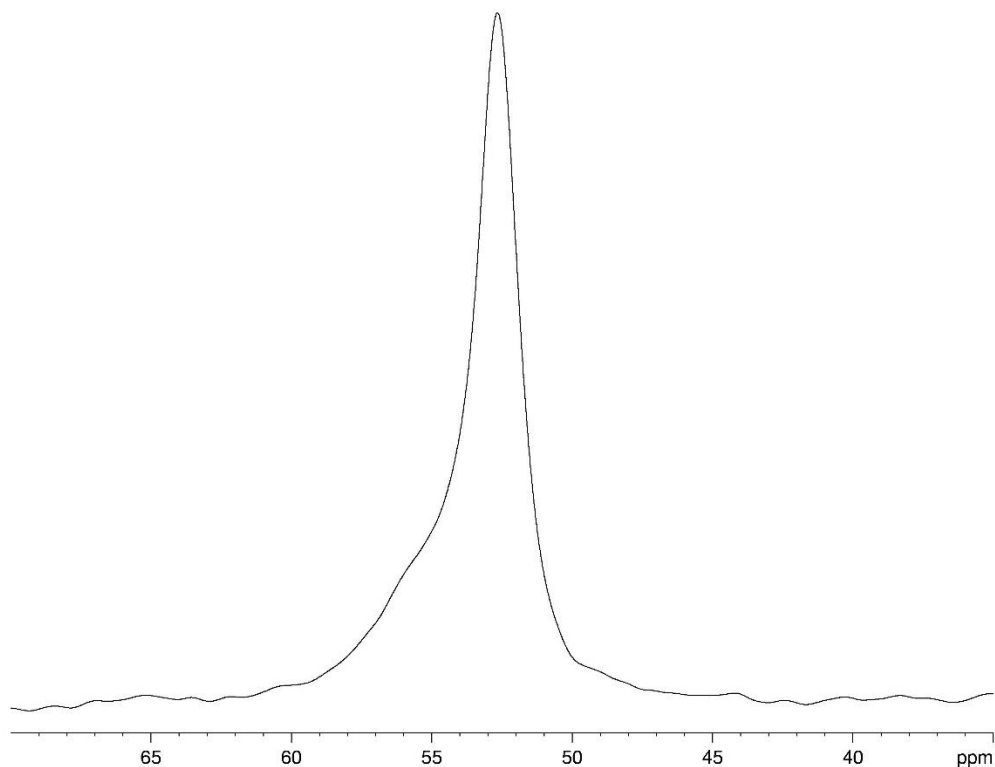


Figure S58. Methoxy signal of  $^1\text{H}$ - $^{13}\text{C}$  CPMAS spectrum ( $t_{\text{cp}} = 3.0$  ms) of TAPB-OMePDA COF

## References

1. Li, X.; Zhang, C.; Cai, S.; Lei, X.; Altoe, V.; Hong, F.; Urban, J. J.; Ciston, J.; Chan, E. M.; Liu, Y. Facile Transformation of Imine Covalent Organic Frameworks into Ultrastable Crystalline Porous Aromatic Frameworks. *Nature Communications* **2018**, 9 (1), 2998.
2. Montalvo-Gonzalez, R. and Ariza-Castolo, A. Molecular Structure of Di-aryl-aldimines by Multinuclear Magnetic Resonance and X-Ray Diffraction. *Journal of Molecular Structure* **2003**, 655, 375-389.
3. Shao, P.; Li, J.; Chen, F.; Ma, L.; Li, Q.; Zhang, M.; Zhou, J.; Yin, A.; Feng, X.; Wang, B. Flexible Films of Covalent Organic Frameworks with Ultralow Dielectric Constants under High Humidity. *Angew. Chem. Int. Ed.* **2018**, 57 (50), 16501–16505.